Hydrodynamic sound modes and viscous damping in a magnon fluid

Joaquin F. Rodriguez-Nieva,[1] Daniel Podolsky,[2,3] and Eugene Demler[1]
[1]*Department of Physics, Harvard University, Cambridge, MA 02138, USA*
[2]*Department of Physics, Technion, Haifa 32000, Israel and*
[3]*ITAMP, Harvard-Smithsonian Center for Astrophysics, Cambridge, Massachusetts 02138, USA*
(Dated: October 31, 2018)

The non-interacting magnon gas description in ferromagnets breaks down at finite magnon density wherein momentum-conserving collisions between magnons become important. Observation of the collision-dominated regime, however, has been hampered by the lack of probes to access the energy and lengthscales characteristic of this regime. Here we identify a key signature of the collision-dominated hydrodynamic regime — a magnon sound mode — which governs dynamics at low frequencies and can be readily detected with recently-introduced spin qubit magnetometers. The magnon sound mode is manifested as an excitation of the longitudinal spin component with frequencies below the spin wave continuum in gapped ferromagnets. At sufficiently large frequencies, the sound mode is damped by viscous forces. The hydrodynamic sound mode, if detected, can lead to a new platform to explore hydrodynamic behavior in quantum materials.

Introduction — The presence of conservation laws can alter the dynamics and transport behavior of interacting quantum systems in dramatic ways. One such example is the recently observed hydrodynamic regime in graphene, wherein fast momentum-conserving collisions lead to viscous electron transport[1–6]. Although vigorous efforts are currently underway in understanding hydrodynamic behavior in a variety of quantum systems, table-top realizations of the hydrodynamic regime, and probes to access them, are still rare.

Here we propose a new platform to study hydrodynamics, namely, an interacting magnon fluid, and an experimental protocol to detect hydrodynamic behavior using spin qubit magnetometers[7, 8]. In particular, we show that a magnon gas describing low-energy excitations in a ferromagnet can enter the hydrodynamic regime in a wide range of temperatures and frequencies. As we argue below, the description of large wavelength excitations in terms of ballistically-propagating magnons, or spin waves, relies on a vanishingly small magnon-magnon collisions which render relaxation processes at the bottom of the band very inefficient. However, as temperature increases and the thermal magnon population occupies larger momentum states, *momentum conserving* collisions give rise to a relaxation length which steeply decreases with temperature:

$$\xi \approx \frac{\lambda a}{z}\left(\frac{J}{T}\right)^{5/2}. \tag{1}$$

Here a is the lattice spacing, T is the temperature, J is the exchange coupling, $z = e^{-\mu/T}$ is the magnon fugacity (μ: chemical potential), and $\lambda \sim 15$ is a numerical prefactor which we estimate below. Although Eq.(1) was obtained for a two-dimensional ferromagnet and $z \ll 1$, the results extrapolates accurately even to $z \approx 1$ (the power of $1/T$ changes to 7/2 in 3D ferromagnets). For an intermediate temperature range such that Umklapp scattering can be neglected ($T \ll J$), but large enough such that $\xi \ll L$ for some characteristic system length L, hydrodynamic behavior emerges. For instance, for a typical ferromagnet ($J \sim 100\,\mathrm{meV}$, $a \sim 0.3\,\mathrm{nm}$) at room temperature $T \sim 25\,\mathrm{meV}$ and $z \approx 1$, the relaxation length $\xi \sim 100\,\mathrm{nm}$ is much smaller than a typical system size.

A key signature of momentum-conserving collisions is the existence of a sound mode. As shown in Fig.1, the sound mode is manifested as an excitation of the longitudinal spin correlator, $\langle \hat{S}^z \hat{S}^z \rangle$, where $\hat{S}^z$ is related to the magnon density n via $\langle \hat{S}^z \rangle = S(1-n)$. As a result, spin fluctuation measurements can provide clear-cut signatures of the sound mode, as shown below.

The hydrodynamic description described here differs from previous descriptions which assume momentum relaxation due to Umklapp scattering ($T \approx J$) or due to disorder, as first described in the seminal work of Halperin and Hohenberg[9]. These momentum-relaxing

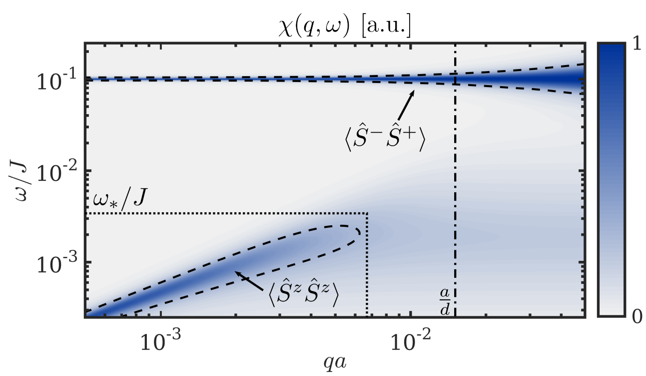

FIG. 1. Spectral function $\chi(q,\omega) = \chi_{+-}(q,\omega) + \chi_{-+}(q,\omega) + 4\chi_{zz}(q,\omega)$ exhbiting single magnon excitations at the Zeeman energy $\Delta = J/10$, induced by a finite $\langle S^- S^+ \rangle$, and a linearly dispersing sound mode at low frequencies induced by magnon density fluctuations, $\langle \hat{S}^z \hat{S}^z \rangle$. The sound mode survives up to frequencies ω_* [see Eq.(18)] wherein viscous forces damp the hydrodynamic excitations.

effects give rise to diffusive particle and energy transport. Although a few authors [10–12] made the case for momentum-conserving hydrodynamic behavior in a magnon gas at the same time as Ref. [9], no experimental signature of this regime has been observed to date. Arguably, the energy scales ($\sim$meV) and wavevectors ($\sim 1/a$) accessible by neutron scattering, the most common probe of ferromagnets at the time, were too large to access the low frequency, long-wavelenth regime in which hydrodynamic sound modes live.

We argue that the conditions for the observation and study of sounds modes have already been met in a recent experiment by C. Du, *et al.*[13]. First, ultraclean ferromagnetic materials, such as Yttrium-Iron-Garnet (YIG), allow ballistic propagation of magnons in macroscopic scales without scattering by impurities. Second, *independent* control of temperature and chemical potential is now possible via a combination of heating and driving and, therefore, enables us to explore all possible regimes from non-interacting magnon gases to interacting magnon fluids. Finally, magnetic spectroscopy with spin qubits allows to access spin fluctuations at the energy and lengthscales relevant for the hydrodynamic sound mode. Besides spin waves[13, 14], such probes have been successfully applied for imaging single spins[15], and domain walls[16], and to study electron transport in metals[17]. The have also been proposed to access the hydrodynamic regime in graphene [18] and one-dimensional systems[19], to study magnon consensation [20] and magnetic monopoles in spin ice[21], and to diagnose ground states in frustrated magnets[22].

Before proceeding to the details of the model, we highlight features of the magnon fluid to distinguish it from its classical and electronic counterparts. First, the collision between magnons is strongly constrained by SU(2) symmetry, giving rise to a strongly momentum dependent magnon-magnon interaction[23, 24], see Eq.(5). Second, rather than sound modes, electron fluids host plasmon modes because longitudinal charge fluctuations are mediated by long-ranged Coulomb interactions[25]. Third, contrary to classical and electron fluids where particles cannot be physically created or annhiliated, conservations laws are not as robust in a magnon fluid and, therefore, should be subject to scrutiny. In particular, magnon number is only conserved approximately due to, for instance, dipolar interactions. As we argue below, because collisions are mediated by exchange coupling $J \sim 100\,\text{meV}$, which is much larger than any other energy scale (or time scale) related to magnon leakage, there is a large window of frequencies were particle number remains conserved and, therefore, the sound mode is a well defined excitation.

Microscopic model — To make direct contact with experiments, we assume a thin film Heisenberg ferromagnet in the presence of an out-of-plane Zeeman field such that, in the temperature range of interest, the system is effectively a 2D magnetically ordered ferromagnet:

$$\hat{\mathcal{H}}_{\rm F} = -J \sum_{\langle jj' \rangle} \hat{\boldsymbol{S}}_j \cdot \hat{\boldsymbol{S}}_{j'} + \Delta \sum_j \hat{S}^z_j. \tag{2}$$

Here j labels the lattice site, $\sum_{\langle jj' \rangle}$ denotes summation over nearest neighbors, and we take periodic boundary conditions in each spatial direction. We assume that the spin system has N lattice sites on a square lattice, each containing a spin S degree of freedom which satisfies the commutation relations $[\hat{S}^z_j, \hat{S}^{\pm}_{j'}] = \pm\delta_{jj'}\hat{S}^{\pm}_j$ and $[\hat{S}^+_j, \hat{S}^-_{j'}] = 2\delta_{jj'}\hat{S}^z_j$, with $\hat{S}^{\pm}_j = \hat{S}^x_j \pm i\hat{S}^y_j$ the raising and lowering spin operators. The Zeeman term is essential to our discussion as it allows to separate the magnon continuum from the gapless sound mode. To leading order, it also allows us to neglect the dynamics of the order parameter. Although the latter can be introduced via emergent gauge fields [26–29] such that magnons can interact with magnetic textures, here we only focus on the manifestations of momentum-conserving collisions.

It is clear from Eq.(2) that energy and total number of spin excitations, or spin flips, is conserved, $[\hat{\mathcal{H}}, \sum_j \hat{S}^z_j] = 0$. Momentum conservation, however, is less obvious. We recall that one magnon states $|\boldsymbol{k}\rangle = \hat{S}^+_{\boldsymbol{k}}|\text{F}\rangle$, where $|\text{F}\rangle = |\downarrow\downarrow \ldots \downarrow\rangle$ is the ferromagnetic ground state and $\hat{S}^+_{\boldsymbol{k}} = \sum_j \frac{e^{-i\boldsymbol{k}\cdot\boldsymbol{r}_j}}{\sqrt{N}} \hat{S}^+_j$, are exact eigenstates of $\hat{\mathcal{H}}_{\rm F}$ with energies

$$\varepsilon_{\boldsymbol{k}} = \Delta + JS(\gamma_0 - \gamma_{\boldsymbol{k}}), \quad \gamma_{\boldsymbol{k}} = \sum_{\boldsymbol{\tau}} e^{i\boldsymbol{k}\cdot\boldsymbol{\tau}}. \tag{3}$$

Two magnon states $|\boldsymbol{k}, \boldsymbol{p}\rangle = \frac{1}{2S}\hat{S}^+_{\boldsymbol{k}}\hat{S}^+_{\boldsymbol{p}}|\text{F}\rangle$, however, are *not* eigenstates of $\hat{\mathcal{H}}_{\rm F}$[23, 24, 30]. Indeed, it is straightforward [31] to show that

$$\begin{aligned} \hat{\mathcal{H}}_{\rm F}|\boldsymbol{k}, \boldsymbol{p}\rangle &= (\varepsilon_{\boldsymbol{k}} + \varepsilon_{\boldsymbol{p}})|\boldsymbol{k}, \boldsymbol{p}\rangle + \sum_{\boldsymbol{q}} g_{\boldsymbol{k},\boldsymbol{p},\boldsymbol{q}}|\boldsymbol{k}+\boldsymbol{q}, \boldsymbol{p}-\boldsymbol{q}\rangle, \\ g_{\boldsymbol{k},\boldsymbol{p},\boldsymbol{q}} &= \frac{J}{N}\left(\gamma_{\boldsymbol{q}} - \gamma_{\boldsymbol{q}-\boldsymbol{p}} - \gamma_{\boldsymbol{q}+\boldsymbol{k}} + \gamma_{\boldsymbol{k}+\boldsymbol{q}-\boldsymbol{p}}\right), \end{aligned} \tag{4}$$

such that one magnon states are coupled via the interaction $g_{\boldsymbol{k},\boldsymbol{p},\boldsymbol{q}}$. When incoming and outgoing magnons are close to the bottom of the band, and considering energy conservation, the collision term takes the form $g_{\boldsymbol{k},\boldsymbol{p},\boldsymbol{q}} \approx \frac{Ja^2}{N}(\boldsymbol{k}\cdot\boldsymbol{p})$. This characteristic $(\boldsymbol{k}\cdot\boldsymbol{p})$ interaction, which arises from the global SU(2) symmetry, justifies why magnons propagate ballistically when $|\boldsymbol{k}| \to 0$.

We can now derive a continuum description of the interacting magnon fluid which captures all the features of the parent Hamiltonian (2), namely, momentum and magnon number conservation and the $(\boldsymbol{k}\cdot\boldsymbol{p})$ dependence of the collision term. If the magnon density is small, $na^2 \ll 1$, we can describe the magnon fluid as a bose gas with kinetic energy $\varepsilon_{\boldsymbol{k}}$, Eq.(3), and the two-body interaction in Eq.(4). Further, close to thermal equilibrium at $T \ll J$, only small $\boldsymbol{k}$ vectors are occupied. As such, we expand the kinetic and interaction terms at low momenta,

$$\hat{\mathcal{H}}_{\rm F} = \sum_{\boldsymbol{k}} \varepsilon_{\boldsymbol{k}} \hat{a}^{\dagger}_{\boldsymbol{k}} \hat{a}_{\boldsymbol{k}} + \frac{Ja^2}{N} \sum_{\boldsymbol{kpq}} (\boldsymbol{k}\cdot\boldsymbol{p}) \hat{a}^{\dagger}_{\boldsymbol{p}+\boldsymbol{q}} \hat{a}^{\dagger}_{\boldsymbol{k}-\boldsymbol{q}} \hat{a}_{\boldsymbol{p}} \hat{a}_{\boldsymbol{k}}, \quad (5)$$

where $\varepsilon_{\boldsymbol{k}} \approx \Delta + \boldsymbol{k}^2/2m$ is the magnon kinetic energy, and $m = 1/2JSa^2$ is the magnon mass. Equation (5) is the starting point for our hydrodynamic theory.

Magnon hydrodynamics — When only magnons close to the bottom of the band are occupied, the scattering matrix elements for magnon collisions can be taken as a small parameter. As a result, a kinetic description of the magnon fluid is suitable, and all thermodynamic and transport coefficients can be computed to leading order in the interaction strength. Our starting point is the kinetic equation,

$$\left[\partial_t + \boldsymbol{v}_{\boldsymbol{k}}\cdot\nabla_{\boldsymbol{r}} + \boldsymbol{F}\cdot\nabla_{\boldsymbol{k}}\right] n_{\boldsymbol{k}}(\boldsymbol{r},t) = \mathcal{I}_{\boldsymbol{k}}, \quad (6)$$

where $n_{\boldsymbol{k}} = \langle \hat{a}^{\dagger}_{\boldsymbol{k}} \hat{a}_{\boldsymbol{k}} \rangle$ is the time-dependent average occupation number of state $\boldsymbol{k}$, $\boldsymbol{F}$ is a fluctuating force, $\boldsymbol{v}_{\boldsymbol{k}} = \boldsymbol{k}/m$ is the magnon velocity, and $\mathcal{I}_{\boldsymbol{k}}$ is the collision integral ($\hbar = 1$):

$$\begin{aligned}\mathcal{I}_{\boldsymbol{k}} = \; & \frac{2\pi}{N^2} \sum_{\boldsymbol{pq}} |\mathcal{M}_{\rm i\to f}|^2 \left[n_{\boldsymbol{k}} n_{\boldsymbol{p}} (1+n_{\boldsymbol{k}+\boldsymbol{q}})(1+n_{\boldsymbol{p}-\boldsymbol{q}}) \right. \\ & \left. -(1+n_{\boldsymbol{k}})(1+n_{\boldsymbol{p}}) n_{\boldsymbol{k}+\boldsymbol{q}} n_{\boldsymbol{p}-\boldsymbol{q}} \right] \delta(\varepsilon_{\rm i} - \varepsilon_{\rm f}).\end{aligned} \quad (7)$$

In Eq.(7), $\mathcal{M}_{\rm i\to f} = Ja^2(\boldsymbol{k}\cdot\boldsymbol{p})$ is the transition matrix element, and $\varepsilon_{\rm i} = \varepsilon_{\boldsymbol{k}} + \varepsilon_{\boldsymbol{p}}$ ($\varepsilon_{\rm f} = \varepsilon_{\boldsymbol{k}+\boldsymbol{q}} + \varepsilon_{\boldsymbol{p}-\boldsymbol{q}}$) is the energy of the initial (final) state of the two-magnon collision. Equation (7) is valid because the thermal length $\xi_{\rm th} = 1/\sqrt{mT}$ is much smaller than the relaxation length, $\xi_{\rm th}/\xi \sim (T/J)^2 \ll 1$ [see Eq.(1)], such that collisions between magnons are independent and, therefore, phase interference effects can be ignored. The quantities of interest are the magnon density n, momentum density $P_\alpha = nmu_\alpha$, and thermal energy $\Theta = n\theta$, defined as

$$\begin{bmatrix} n \\ P_\alpha \\ \Theta \end{bmatrix} = \int \frac{d\boldsymbol{k}}{(2\pi)^2} \begin{bmatrix} 1 \\ v_{\boldsymbol{k},\alpha} \\ \theta_{\boldsymbol{k}} \end{bmatrix} n_{\boldsymbol{k}}(\boldsymbol{r},t), \quad (8)$$

where $\theta_{\boldsymbol{k}} = m\tilde{\boldsymbol{v}}^2_{\boldsymbol{k}}/2$, and $\tilde{v}_{\boldsymbol{k},\alpha} = v_{\boldsymbol{k},\alpha} - u_\alpha$ is the relative velocity. Thermodynamic equilibrium ($\mathcal{I}_{\boldsymbol{k}} = 0$) is guaranteed by the distribution function

$$\bar{n}_{\boldsymbol{k}}(T,z,w_\alpha) = \frac{1}{z^{-1}e^{\theta_{\boldsymbol{k}}/T} - 1}, \quad \theta_{\boldsymbol{k}} = \frac{m}{2}(\boldsymbol{v}_{\boldsymbol{k}} - \boldsymbol{w})^2, \quad (9)$$

with thermodynamic potentials (T, z, w_α), with z defined $z = e^{-\mu/T}$. We stress again that z can be controlled independently of T in the presence of driving. The values of (n, u_α, θ) in thermal equilibrium are given by

$$\bar{n} = \frac{mT}{2\pi} g_1(z), \qquad \bar{u}_\alpha = w_\alpha, \qquad \bar{\theta} = \frac{Tg_2(z)}{g_1(z)}. \quad (10)$$

Here $g_\nu(z)$ is the Bose integral, $g_\nu(z) = \frac{1}{\Gamma(\nu)}\int_0^\infty \frac{dy y^{\nu-1}}{e^y/z-1}$, with $\Gamma(\nu)$ the Gamma function. In what follows, we will focus on an equilibrium distribution with $w_\alpha = 0$.

Fluctuations of the distribution function $n_{\boldsymbol{k}} = \bar{n}_{\boldsymbol{k}} + \delta n_{\boldsymbol{k}}$ lead to particle number, momentum, and energy currents, given by

$$\begin{aligned} J_\alpha &= nu_\alpha, \\ \Pi_{\alpha\beta} &= mnu_\alpha u_\beta + mP_{\alpha\beta}, \;\; P_{\alpha\beta} = \int \frac{d\boldsymbol{k}}{(2\pi)^2} \tilde{v}_{\boldsymbol{k},\alpha} \tilde{v}_{\boldsymbol{k},\beta} n_{\boldsymbol{k}}, \\ Q_\alpha &= n\theta u_\alpha + q_\alpha, \qquad\quad q_\alpha = \int \frac{d\boldsymbol{k}}{(2\pi)^2} \theta_{\boldsymbol{k}} \tilde{v}_{\boldsymbol{k},\alpha} n_{\boldsymbol{k}}, \end{aligned} \quad (11)$$

respectively, with $P_{\alpha\beta}$ the pressure tensor, and q_α the heat current. The continuity equation for each of the quantities $\eta_j = (n, u_\alpha, \theta)$, $\dot{\eta}_j + \nabla_{\boldsymbol{r}}\cdot\boldsymbol{J}_{\eta_j} = \mathcal{F}_{\eta_j}$, with $\mathcal{F}_{\eta_j} = \int \frac{d\boldsymbol{k}}{(2\pi)^2} (\boldsymbol{F}\cdot\nabla_{\boldsymbol{k}}\eta_j)\bar{n}_{\boldsymbol{k}}$ yield the hydrodynamic equations

$$\begin{aligned} &\dot{n} + \partial_\alpha(nu_\alpha) = 0, \\ &\dot{u}_\beta + u_\alpha\partial_\alpha u_\beta = \frac{F_\beta}{m} - \frac{1}{n}\partial_\alpha P_{\alpha\beta}, \\ &\dot{\theta} + u_\alpha\partial_\alpha\theta = -\frac{1}{n}\partial_\alpha q_\alpha - \frac{1}{n}P_{\alpha\beta}\partial_\alpha u_\beta. \end{aligned} \quad (12)$$

We estimate dissipation effects within the relaxation time approximation. This approximation allows to relate the nonequilibrium magnon density to gradients in $\eta_j = (n, u_\alpha, \theta)$, $n_{\boldsymbol{k}} = \bar{n}_{\boldsymbol{k}} + \tau_{\boldsymbol{k}} \sum_j (\partial\bar{n}_{\boldsymbol{k}}/\partial\eta_j)(\partial_t + \boldsymbol{v}_{\boldsymbol{k}}\cdot\nabla_{\boldsymbol{r}})\eta_j$, where $\tau_{\boldsymbol{k}}$ is a characteristic relaxation time defined as $\frac{1}{\tau_{\boldsymbol{k}}} = \frac{\delta\mathcal{I}_{\boldsymbol{k}}}{\delta n_{\boldsymbol{k}}} = \gamma_{\boldsymbol{k}}(z)T^2(ka)^2/J$. As shown in the Supplement[31], the dimensionless function $\gamma_{\boldsymbol{k}}(z)$ depends weakly on $\boldsymbol{k}$ and can be well approximated as $\gamma(z) \approx cz$, with $c \sim 0.1$. The relaxation length in Eq.(1) can be obtained from $\xi = k_{\rm th}\tau_{k_{\rm th}}/m$, where $k_{\rm th} = \sqrt{2Tg_2(z)/mg_1(z)}$ is the thermal momentum. Expressing $\delta n_{\boldsymbol{k}}$ in terms of gradients of (n, u_α, θ), assuming that they are small, and using cylindrical symmetry, allows us to write $P_{\alpha\beta}$ and q_α as

$$\begin{aligned} P_{\alpha\beta} &= \tfrac{n\theta}{m}\delta_{\alpha\beta} + \mu\left(\partial_\alpha u_\beta + \partial_\beta u_\alpha - \delta_{\alpha\beta}\partial_\gamma u_\gamma\right), \\ q_\alpha &= \kappa_n\partial_\alpha n + \kappa_\theta\partial_\alpha\theta. \end{aligned} \quad (13)$$

In the case of a two-dimensional magnon gas with quadratic dispersion and collision rate of the form $1/\tau_{\boldsymbol{k}} \propto \boldsymbol{k}^2$, we find [31] that, within the relaxation time approximation, dissipation is dominated by the viscous effects $\mu(T,z) = \frac{\pi}{2}\frac{g_1(z)}{\gamma(z)}\frac{J^2}{T}$, whereas particle and energy diffusion are second order effects dominated, for instance, by deviation from quadratic dispersion; as such, we set $q_\alpha \to 0$.

The sound mode becomes evident when computing response functions. Because we are interested in spin fluctuations, which are directly accessible with noise magnetometry, here we focus on longitudinal spin fluctuations as quantified by the retarded correlator

$$\chi_{zz}(\boldsymbol{q},\omega) = -i\int_0^\infty dt e^{i\omega t} \sum_{\boldsymbol{\tau}} e^{-i\boldsymbol{q}\cdot\boldsymbol{\tau}} \langle [\hat{S}^z_i(t), \hat{S}^z_{i+\tau}(0)] \rangle, \quad (14)$$

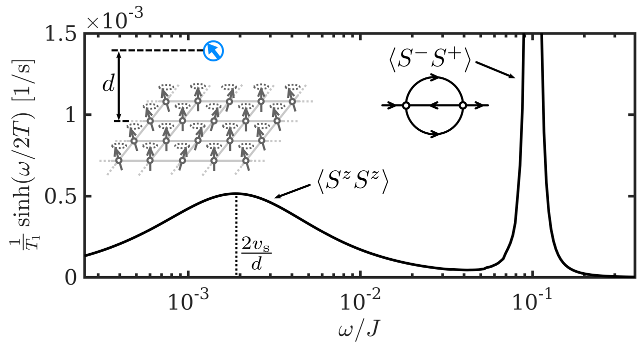

FIG. 2. Relaxation time [normalized by $\sinh(\omega/2T)$] of a spin qubit located a distance d from the 2D ferromagnet. Besides the characteristically large relaxation rate induced by spin relaxation due to emission of spin waves at energy Δ, the relaxation rate exhibits a peak below the ferromagentic gap induced by emission of sound modes with velocity $v_{\rm s}$. Parameters used: $z = 0.9$, $T/J = 0.2$, $\Delta/J = 0.1$, $a = 0.3\,$nm, and $d = 20\,$nm.

which is equivalent to computing density fluctuation because $\hat{S}^z_i = -S(1-\hat{n}_i)$. In thermal equilibrium, the fluctuation amplitude can be computed from the response function due to an external force $\boldsymbol{F}$, see Eq.(12). With this objective in mind, we first linearize hydrodynamic equations around the equilibrium values, $n(\boldsymbol{r},t) = \bar{n} + \delta n(\boldsymbol{r},t)$, $\theta(\boldsymbol{r},t) = \bar{\theta} + \delta\theta(\boldsymbol{r},t)$, and $u_\alpha(\boldsymbol{r},t) = \delta u_\alpha(\boldsymbol{r},t) \ll \sqrt{T/m}$, and go to momentum space:

$$\begin{pmatrix} \omega & -\bar{n}q & 0 \\ -\bar{\theta}q/m\bar{n} & \omega + i\mu q^2/\bar{n} & -q/m \\ 0 & -\bar{\theta}q & \omega \end{pmatrix} \begin{pmatrix} \delta n \\ \delta p_\parallel \\ \delta\theta \end{pmatrix} = \begin{pmatrix} 0 \\ iF_\parallel \\ 0 \end{pmatrix}. \tag{15}$$

Here we defined $\delta p_\parallel = m\delta u_\parallel$ as the longitudinal momentum which is coupled to δn and $\delta\theta$, and gives rise to two propagating modes and one diffusive mode. The transverse momentum component, $\delta p_\perp$, which does not couple to δn, gives rise to a diffusive mode, $(\omega + i\mu q^2/\bar{n})\delta p_\perp = iF_\perp$. From Eq.(15), it is straight-forward to compute the response function and derive the density-density correlator:

$$\chi_{zz}(q,\omega) = \frac{JS^2(\bar{n}qa^2)^2}{\omega^2 - 2\bar{\theta}q^2/m + i\mu\omega q^2/\bar{n}}, \tag{16}$$

which exhibits a linearly dispersing sound mode:

$$\omega = v_{\rm s}q, \quad v_{\rm s} = a\sqrt{2JTg_2(z)/g_1(z)}. \tag{17}$$

The sound mode survives up to a temperature and chemical-potential-dependent frequency ω_*, given by

$$\omega_* = \frac{2\gamma(z)}{\pi^2}\frac{g_2(z)}{g_1(z)}\frac{T^3}{J^2}, \tag{18}$$

above which it gets damped by viscous forces.

Detection of the sound mode — We consider a spin-1/2 qubit with an intrinsic level splitting ω placed a distance d above the magnetic insulator. The combined dynamics of the qubit and ferromagnet is governed by the Hamiltonian $\hat{\mathcal{H}} = \hat{\mathcal{H}}_{\rm F} + \hat{\mathcal{H}}_{\rm F-q} + \hat{\mathcal{H}}_{\rm q}$, where $\hat{\mathcal{H}}_{\rm F}$ was defined in Eq.(2), and $\hat{\mathcal{H}}_{\rm q}$ is the spin qubit Hamiltonian $\hat{\mathcal{H}}_{\rm q} = \frac{1}{2}\omega\sigma_z$ with polarizing field assumed to be aligned in the z direction. The term $\hat{\mathcal{H}}_{\rm F-q}$ is the qubit-ferromagnet coupling induced by dipolar interactions:

$$\hat{\mathcal{H}}_{\rm F-q} = \frac{\mu_{\rm B}^2}{2}\hat{\boldsymbol{\sigma}}\cdot\hat{\boldsymbol{B}}, \quad \hat{\boldsymbol{B}} = \frac{1}{4\pi}\sum_j\left[\frac{\hat{\boldsymbol{S}}_j}{r_j^3} - \frac{3(\hat{\boldsymbol{S}}_j\cdot\boldsymbol{r}_j)\boldsymbol{r}_j}{r_j^5}\right], \tag{19}$$

where $\boldsymbol{r}_j = (x_j, y_j, -d)$ is the relative position between the i-th spin in the 2D lattice and probe. The relaxation time of the spin qubit can be obtained from Fermi Golden's rule[31]:

$$\frac{1}{T_1} = \frac{\mu_{\rm B}^2}{2}\int_{-\infty}^{\infty} dt e^{i\omega t}\langle\{\hat{B}^-(t), \hat{B}^+(0)\}\rangle, \tag{20}$$

where $\{,\}$ denotes anticommutation. Replacing Eq.(19) into Eq.(20) and using the fluctuation-dissipation theorem, the relaxation time can be expressed in terms of spin correlation functions:

$$\begin{aligned}\frac{1}{T_1} = \ &\coth\left(\frac{\omega}{2T}\right)\frac{\mu_{\rm B}^2}{2a^2}\int\frac{d^2\boldsymbol{q}}{(2\pi)^2}e^{-2|\boldsymbol{q}|d}|\boldsymbol{q}|^2\left[\chi''_{-+}(\boldsymbol{q},\omega)\right.\\ &\left.+\chi''_{+-}(\boldsymbol{q},\omega) + 4\chi''_{zz}(\boldsymbol{q},\omega)\right],\end{aligned} \tag{21}$$

where we denote $\chi''_{\alpha\beta} = -{\rm Im}[\chi_{\alpha\beta}]$, and $\chi^{\rm R}_{\alpha\beta}(\boldsymbol{q},\omega) = -i\int_0^\infty dt\langle[\hat{S}^\alpha_{-\boldsymbol{q}}(t), \hat{S}^\beta_{\boldsymbol{q}}(0)]\rangle$. Figure 1 shows the integrand of Eq.(21), and Fig.2 shows the spin relaxation time as a function of ω induced by longitudinal and transverse spin fluctuations (we assumed a constant magnon population $\bar{n}$ and T). The correlators $\chi_{\pm\mp}(\boldsymbol{q},\omega)$ are related to single-magnon production/absorption, which we assume to be given by $\chi^{-1}_{+-}(\boldsymbol{q},\omega) = \omega - \omega_{\boldsymbol{q}} + i\Sigma''(\boldsymbol{q},\omega)$, where $\Sigma''(\boldsymbol{q},\omega) \sim \frac{T\omega}{J}(qa)^2$ (valid for $z \sim 1$ and $\omega \ll T$) is the imaginary part of the self-energy computed from the sunrise diagram, see inset of Fig.2 and details in [31]. We also note that, in Fig.2, we normalize $1/T_1$ with $\coth(\omega/2T)$ to capture the spectral contribution of spin fluctuations rather than its amplitude.

Figure 2 is the main result of this work, and shows a clear fingerprint of the sound mode within the gap of the ferromagnet. Because of the distance dependence of the dipolar interaction introduced by the term $|\boldsymbol{q}|^2e^{-2|\boldsymbol{q}|d}$ in Eq.(21), the frequency of the peak in Fig.2 depends on the inverse qubit-sample distance d.

Dipolar interactions — Dipolar interactions is one important mechanism of magnon decay via three-magnon processes, particularly in thin layers with a canted ferromagnetic order parameter. Assuming the steady-state distribution in Eq.(9), we can estimate the typical magnon decay time induced by a dipolar term $\hat{\mathcal{H}}_{\rm d} = \frac{g_{\rm d}}{2}\sum_{jj'}\left[\frac{\hat{\boldsymbol{S}}_j\cdot\hat{\boldsymbol{S}}_{j'}}{r^3_{jj'}} - \frac{3(\hat{\boldsymbol{S}}_j\cdot\boldsymbol{r}_{jj'})(\hat{\boldsymbol{S}}_{j'}\cdot\boldsymbol{r}_{jj'})}{r^5_{jj'}}\right]$, with $g_{\rm d} = \mu_{\rm B}^2/4\pi$.

This gives values [31] on the ballpark $\frac{1}{\bar{n}}\frac{d\bar{n}}{dt} \sim \frac{g_4^2}{J}(z^2 - z^3) \sim$ MHz, several orders of magnitude smaller than the typical GHz frequencies that typical spin-qubit magnetometers can access. As a result, sound modes are expected to be well defined excitations in a wide range of frequencies, from MHz to several GHz.

Conclusion — Our predictions, which can be tested in current experiments using spin qubit magnetometers, provide distinct signatures of momentum conserving hydrodynamics in ferromagnets. Although the sound mode is its most distinctive feature, the strong momentum dependence of the magnon-magnon interaction suggests that ferromagnets can also host anomalous hydrodynamic behavior not achievable in classical and electron fluids.

Acknowledgements — We acknowledge insightful discussions with D. Abanin, T. Andersen, C. Du, M. .D. Lukin, A. Rosch, A. Yacoby, J. Sanchez-Yamagishi, and T. Zhou. JFRN and ED acknowledge support from Harvard-MIT CUA, NSF Grant No. DMR-1308435 and AFOSR-MURI: Photonic Quantum Matter (award FA95501610323). DP thanks support by the Joint UGS-ISF Research Grant Program under grant number 1903/14 and by the National Science Foundation through a grant to ITAMP at the Harvard-Smithsonian Center for Astrophysics.

[1] I. Torre, A. Tomadin, A. K. Geim, and M. Polini, Phys. Rev. B **92**, 165433 (2015).

[2] D. A. Bandurin, I. Torre, R. K. Kumar, M. Ben Shalom, A. Tomadin, A. Principi, G. H. Auton, E. Khestanova, K. S. Novoselov, I. V. Grigorieva, L. A. Ponomarenko, A. K. Geim, and M. Polini, Science **351**, 1055 (2016).

[3] J. Crossno, J. K. Shi, K. Wang, X. Liu, A. Harzheim, A. Lucas, S. Sachdev, P. Kim, T. Taniguchi, K. Watanabe, T. A. Ohki, and K. C. Fong, Science **351**, 1058 (2016).

[4] L. Levitov and G. Falkovich, Nature Physics **12**, 672 (2016).

[5] H. Guo, E. Ilseven, G. Falkovich, and L. S. Levitov, Proceedings of the National Academy of Sciences **114**, 3068 (2017).

[6] R. Krishna Kumar, D. A. Bandurin, F. M. D. Pellegrino, Y. Cao, A. Principi, H. Guo, G. Auton, M. Ben Shalom, L. A. Ponomarenko, G. Falkovich, K. Watanabe, T. Taniguchi, I. Grigorieva, L. S. Levitov, M. Polini, and A. Geim, Nature Physics **13**, 1182 (2017).

[7] L. Rondin, J.-P. Tetienne, T. Hingant, J.-F. Roch, P. Maletinsky, and V. Jacques, Reports on Progress in Physics **77**, 056503 (2014).

[8] C. L. Degen, F. Reinhard, and P. Cappellaro, Rev. Mod. Phys. **89**, 035002 (2017).

[9] B. I. Halperin and P. C. Hohenberg, Phys. Rev. **188**, 898 (1969).

[10] G. F. Reiter, Phys. Rev. **175**, 631 (1968).

[11] K. Michel and F. Schwabl, Solid State Communications **7**, 1781 (1969).

[12] F. Schwabl and K. H. Michel, Phys. Rev. B **2**, 189 (1970).

[13] C. Du, T. van der Sar, T. X. Zhou, P. Upadhyaya, F. Casola, H. Zhang, M. C. Onbasli, C. A. Ross, R. L. Walsworth, Y. Tserkovnyak, and A. Yacoby, Science **357**, 195 (2017).

[14] T. van der Sar, F. Casola, R. Walsworth, and A. Yacoby, Nat Commun (2015).

[15] M. S. Grinolds, S. Hong, P. Maletinsky, L. Luan, M. D. Lukin, R. L. Walsworth, and A. Yacoby, Nat Phys **9**, 215 (2013).

[16] J.-P. Tetienne, T. Hingant, L. Martnez, S. Rohart, A. Thiaville, L. H. Diez, K. Garcia, J.-P. Adam, J.-V. Kim, J.-F. Roch, I. Miron, G. Gaudin, L. Vila, B. Ocker, D. Ravelosona, and V. Jacques, Nat Commun (2015).

[17] S. Kolkowitz, A. Safira, A. A. High, R. C. Devlin, S. Choi, Q. P. Unterreithmeier, D. Patterson, A. S. Zibrov, V. E. Manucharyan, H. Park, and M. D. Lukin, Science **347**, 1129 (2015).

[18] K. Agarwal, R. Schmidt, B. Halperin, V. Oganesyan, G. Zaránd, M. D. Lukin, and E. Demler, Phys. Rev. B **95**, 155107 (2017).

[19] J. F. Rodriguez-Nieva, K. Agarwal, T. Giamarchi, B. I. Halperin, M. D. Lukin, and E. Demler, arXiv:1803.01521.

[20] B. Flebus and Y. Tserkovnyak, arXiv:1804.02417.

[21] F. K. K. Kirschner, F. Flicker, A. Yacoby, N. Y. Yao, and S. J. Blundell, Phys. Rev. B **97**, 140402 (2018).

[22] S. Chatterjee, J. F. Rodriguez-Nieva, and E. Demler, arXiv:1810.04183.

[23] F. J. Dyson, Phys. Rev. **102**, 1217 (1956).

[24] D. C. Mattis, *The Theory of Magnetism Made Simple* (World Scientific, 2006).

[25] A. Lucas and S. Das Sarma, Phys. Rev. B **97**, 115449 (2018).

[26] V. K. Dugaev, P. Bruno, B. Canals, and C. Lacroix, Phys. Rev. B **72**, 024456 (2005).

[27] D. D. Sheka, I. A. Yastremsky, B. A. Ivanov, G. M. Wysin, and F. G. Mertens, Phys. Rev. B **69**, 054429 (2004).

[28] Y.-Q. Li, Y.-H. Liu, and Y. Zhou, Phys. Rev. B **84**, 205123 (2011).

[29] K. A. van Hoogdalem, Y. Tserkovnyak, and D. Loss, Phys. Rev. B **87**, 024402 (2013).

[30] In fact, not only is $|\boldsymbol{k},\boldsymbol{p}\rangle = S^+_{\boldsymbol{k}} S^+_{\boldsymbol{p}}|\mathrm{F}\rangle$ not diagonal, but they are not properly normalized nor do they form an orthogonal basis, see discussion in Supplement.

[31] Supplementary information.

Supplement for 'Hydrodynamic sound modes and viscous damping in a magnon fluid'

Joaquin F. Rodriguez-Nieva,[1] Daniel Podolsky,[2,3] and Eugene Demler[1]
[1]*Department of Physics, Harvard University, Cambridge, MA 02138, USA*
[2]*Department of Physics, Technion, Haifa 32000, Israel*
[3]*ITAMP, Harvard-Smithsonian Center for Astrophysics, Cambridge, Massachusetts 02138, USA*

The outline of the Supplement is as follows. In Sec. A, we show a derivation of the two magnon collision term of the Heisenberg model which follows closely Ref. [24]. In Sec. B, we numerically evaluate the magnon relaxation time due to exchange coupling. In Sec. C, we compute the viscocity of the magnon fluid using the relaxation time approximation. In Sec. D, we evaluate the sunrise diagram which gives rise to a finite linewidth to the single magnon emission/absorption process. In Sec. E, we provide the computational steps to obtain Eq.(21) of the main text. Finally, in Sec. F, we provide a detailed discussion of dipole-dipole interactions and estimate the typical magnon leakage rate.

A. EIGENSTATES OF THE HEISENBERG FERROMAGNET

To illustrate the origin of the collision term in Eq.(4), here we calculate the eigenstates of the Heisenberg Hamiltonian for increasing magnon number. The discussion closely follows that in Ref. [24]. Given that $[\hat{\mathcal{H}}, \sum_i S_i^z] = 0$, we can label eigenstates with the total number of spin flips. Before computing the eigenstates, it is useful to first write the Hamiltonian in momentum space,

$$\hat{\mathcal{H}} = -\frac{J}{4}\sum_{\boldsymbol{k}} \gamma_{\boldsymbol{k}} \left[\hat{S}^+_{-\boldsymbol{k}}\hat{S}^-_{\boldsymbol{k}} + \hat{S}^-_{-\boldsymbol{k}}\hat{S}^+_{\boldsymbol{k}} + 2\hat{S}^z_{-\boldsymbol{k}}\hat{S}^z_{\boldsymbol{k}}\right] + \Delta\sum_j S_j^z, \quad \gamma_{\boldsymbol{k}} = \sum_j e^{i\boldsymbol{k}\cdot\boldsymbol{\tau}}, \tag{S1}$$

where $\boldsymbol{\tau}$ labels the four nearest neighbor vectors. The spin operators in momentum space satisfy the commutation relations $\left[\hat{S}^z_{\boldsymbol{k}}, \hat{S}^\pm_{\boldsymbol{k}'}\right] = \pm\frac{\hat{S}^\pm_{\boldsymbol{k}+\boldsymbol{k}'}}{\sqrt{N}}$, $\left[\hat{S}^+_{\boldsymbol{k}}, \hat{S}^-_{\boldsymbol{k}'}\right] = \frac{2\hat{S}^z_{\boldsymbol{k}+\boldsymbol{k}'}}{\sqrt{N}}$.

Ferromagnetic ground state

The ferromagnetic ground states of $\hat{\mathcal{H}}$ is given by $|F\rangle = |\downarrow\downarrow\ldots\downarrow\downarrow\rangle$ such that all spins are pointing in the $\hat{z}$-direction. The energy of the ferromagnetic ground state is

$$\hat{\mathcal{H}}|F\rangle = E_F|F\rangle, \quad E_F = -2NJS^2 - N\Delta. \tag{S2}$$

Furthermore, the ground state satisfies $\hat{S}^-_j|F\rangle = 0$, and $\hat{S}^z_j|F\rangle = -S|F\rangle$. In momentum space, these two relations become

$$\hat{S}^-_{\boldsymbol{k}}|F\rangle = 0, \quad \hat{S}^z_{\boldsymbol{k}}|F\rangle = -S\sqrt{N}\delta_{\boldsymbol{k},0}|F\rangle. \tag{S3}$$

One magnon eigenstates

There is a total of N possible ways to do a single spin flip over the ferromagnetic ground state, $S_i^+|F\rangle$ for $i = 1,\ldots,N$, giving rise to a total of N one-magnon eigenstates. Single magnon eigenstates of $\hat{\mathcal{H}}$ are *exactly* given by $|\boldsymbol{k}\rangle = \hat{S}^+_{\boldsymbol{k}}|F\rangle$. To show that this is the case, we note that $\hat{\mathcal{H}}\hat{S}^+_{\boldsymbol{k}}|F\rangle = [\hat{S}^+_{\boldsymbol{k}}\hat{\mathcal{H}} + \hat{R}_{\boldsymbol{k}}]|F\rangle$, where

$$\hat{R}_{\boldsymbol{p}} = [\hat{\mathcal{H}}, \hat{S}^+_{\boldsymbol{p}}] = \frac{J}{\sqrt{N}}\sum_{\boldsymbol{q}}(\gamma_{\boldsymbol{p}} - \gamma_{\boldsymbol{p}-\boldsymbol{q}})\left[\hat{S}^z_{\boldsymbol{q}}\hat{S}^+_{\boldsymbol{p}-\boldsymbol{q}} - \hat{S}^+_{\boldsymbol{q}}\hat{S}^z_{\boldsymbol{p}-\boldsymbol{q}}\right] + \Delta S^+_{\boldsymbol{p}}. \tag{S4}$$

Using Eq.(S3), it can be shown that $\hat{R}_{\boldsymbol{k}}|F\rangle = [\Delta + JS(\gamma_0 - \gamma_{\boldsymbol{k}})]\hat{S}^+_{\boldsymbol{k}}|F\rangle$. As a result,

$$\hat{\mathcal{H}}\hat{S}^+_{\boldsymbol{k}}|F\rangle = [E_F + \varepsilon_{\boldsymbol{k}}]\hat{S}^+_{\boldsymbol{k}}|F\rangle, \quad \varepsilon_{\boldsymbol{k}} = \Delta + JS(\gamma_0 - \gamma_{\boldsymbol{k}}), \tag{S5}$$

and, therefore, $|\boldsymbol{k}\rangle = \hat{S}^+_{\boldsymbol{k}}|F\rangle$ is an eigenstate of the Hamiltonian with energy $\varepsilon_{\boldsymbol{k}}$ over the vacuum energy. Because $\langle\boldsymbol{k}|\boldsymbol{p}\rangle = \delta_{\boldsymbol{k},\boldsymbol{p}}$, the one magnon eigenstates $|\boldsymbol{k}\rangle = \hat{S}^+_{\boldsymbol{k}}|F\rangle$ are properly normalized.

Two magnon eigenstates

Spin wave theory assumes that M magnon eigenstates are superposition of M one-magnon eigenstates, for instance

$$|\boldsymbol{k},\boldsymbol{p}\rangle = \frac{1}{\sqrt{2SM_{\boldsymbol{k}}}\sqrt{2SM_{\boldsymbol{p}}}}\hat{S}^+_{\boldsymbol{k}}\hat{S}^+_{\boldsymbol{p}}|F\rangle, \tag{S6}$$

for $M_{\boldsymbol{k}} + M_{\boldsymbol{p}} = 2$. Such a basis has several problems, even in the simplest case $M = 2$. First, the two-magnon basis in Eq.(S6) is overcomplete for $S = 1/2$. In particular, for $S = 1/2$, there is a total of $N(N-1)/2$ ways to do two spin flips on the lattice, giving rise to $N(N-1)/2$ two-magnon eigenstates of $\hat{\mathcal{H}}$. However, there are in total $N(N+1)/2$ ways in which $\boldsymbol{k},\boldsymbol{p}$ pairs of momenta can be chosen. Such problem does not arise for $S > 1/2$, as there is a total of $N(N+1)/2$ ways to do two spin flips on the lattice.

Secondly, the two-magnon basis in Eq.(S6) is neither orthogonal nor properly normalized. Indeed, the scalar product of two elements of the basis is given by

$$\langle F|\hat{S}^-_{-\boldsymbol{p}'}\hat{S}^-_{-\boldsymbol{k}'}\hat{S}^+_{\boldsymbol{k}}\hat{S}^+_{\boldsymbol{p}}|F\rangle = (2S)^2(\delta_{\boldsymbol{k},\boldsymbol{k}'}\delta_{\boldsymbol{p},\boldsymbol{p}'} + \delta_{\boldsymbol{k},\boldsymbol{p}'}\delta_{\boldsymbol{p},\boldsymbol{k}'} - \delta_{\boldsymbol{k}+\boldsymbol{p},\boldsymbol{k}'+\boldsymbol{p}'}/N), \tag{S7}$$

for $S = 1/2$, and

$$\langle F|\hat{S}^-_{-\boldsymbol{p}'}\hat{S}^-_{-\boldsymbol{k}'}\hat{S}^+_{\boldsymbol{k}}\hat{S}^+_{\boldsymbol{p}}|F\rangle = (2S)^2(\delta_{\boldsymbol{k},\boldsymbol{k}'}\delta_{\boldsymbol{p},\boldsymbol{p}'} + \delta_{\boldsymbol{k},\boldsymbol{p}'}\delta_{\boldsymbol{p},\boldsymbol{k}'}) + 4S(S-1)\delta_{\boldsymbol{k}+\boldsymbol{p},\boldsymbol{k}'+\boldsymbol{p}'}/N, \tag{S8}$$

for $S > 1/2$. As a result, orthogonality and normalization of the two magnon basis (S6) is valid up to terms $\mathcal{O}(1/N)$.

Finally, and crucial for our discussion, the two-magnon basis (S6) is not an eigenstate of the Heisenberg Hamiltonian. In particular, the effect of acting $\hat{\mathcal{H}}$ on a two magnon state $\hat{S}^+_{\boldsymbol{p}}\hat{S}^+_{\boldsymbol{k}}|F\rangle$ is given by

$$\hat{\mathcal{H}}\hat{S}^+_{\boldsymbol{p}}\hat{S}^+_{\boldsymbol{k}}|F\rangle = \left[\hat{S}^+_{\boldsymbol{p}}\hat{S}^+_{\boldsymbol{k}}\mathcal{H} + \hat{S}^+_{\boldsymbol{p}}\hat{R}_{\boldsymbol{k}} + \hat{S}^+_{\boldsymbol{k}}\hat{R}_{\boldsymbol{p}}\right]|F\rangle + \hat{Q}_{\boldsymbol{pk}}|F\rangle, \tag{S9}$$

where we defined

$$\hat{Q}_{\boldsymbol{pk}} = \left[\left[\hat{\mathcal{H}}_J, \hat{S}^+_{\boldsymbol{p}}\right], \hat{S}^+_{\boldsymbol{k}}\right] = \frac{J}{N}\sum_{\boldsymbol{q}}\left(\gamma_{\boldsymbol{q}} - \gamma_{\boldsymbol{q}-\boldsymbol{p}} - \gamma_{\boldsymbol{q}+\boldsymbol{k}} + \gamma_{\boldsymbol{q}-\boldsymbol{p}+\boldsymbol{k}}\right)\hat{S}^+_{\boldsymbol{k}+\boldsymbol{q}}\hat{S}^+_{\boldsymbol{p}-\boldsymbol{q}}. \tag{S10}$$

Using Eq.(S3), we find that

$$\hat{\mathcal{H}}\hat{S}^+_{\boldsymbol{p}}\hat{S}^+_{\boldsymbol{k}}|F\rangle = \left[E_F + JS(\gamma_0 - \gamma_{\boldsymbol{k}}) + JS(\gamma_0 - \gamma_{\boldsymbol{p}})\right]\hat{S}^+_{\boldsymbol{p}}\hat{S}^+_{\boldsymbol{k}}|F\rangle + \hat{Q}_{\boldsymbol{pk}}|F\rangle, \tag{S11}$$

where the first term on the right-hand side is the usual spin wave contribution which is diagonal on the two-magnon basis in Eq.(S6). The second term ($\hat{Q}_{\boldsymbol{pk}}$), however, creates two magnon states with momenta $\boldsymbol{p}+\boldsymbol{q}$ and $\boldsymbol{k}-\boldsymbol{q}$, for all $\boldsymbol{q}$. As a result, different two-magnon states are coupled by the matrix elements

$$\langle F|\hat{S}^-_{\boldsymbol{k}+\boldsymbol{q}}\hat{S}^-_{\boldsymbol{p}-\boldsymbol{q}}\hat{\mathcal{H}}\hat{S}^+_{\boldsymbol{k}}\hat{S}^+_{\boldsymbol{p}}|F\rangle = \frac{J}{N}\left(\gamma_{\boldsymbol{q}} - \gamma_{\boldsymbol{q}-\boldsymbol{p}} - \gamma_{\boldsymbol{q}+\boldsymbol{k}} + \gamma_{\boldsymbol{q}-\boldsymbol{p}+\boldsymbol{k}}\right) \approx \frac{Ja^2}{N}(\boldsymbol{k}\cdot\boldsymbol{p}), \tag{S12}$$

where we evaluated the matrix elements at low momenta.

Rather than dealing with the complications introduced by the two-magnon basis described above, it is possible to calculate exactly the two-magnon eigenstate and compute the matrix element in terms of single magnon eigenstates $|\boldsymbol{k}\rangle$. This provides a minimal description of the interacting magnon fluid at small densities, $na^2 \ll 1$. The wavefunction for two-magnon states can be generically written as

$$|\psi\rangle = \sum_{ij}\psi_{i,j}\hat{S}^+_i\hat{S}^+_j|F\rangle, \tag{S13}$$

where $\psi_{i,j} = \psi_{j,i}$. In the case $S = 1/2$, we do not need to explicitly set $\psi_{i,i} = 0$ because $\hat{S}^+_i\hat{S}^+_i|F\rangle$ already gives 0. We look for eigenstates of $\hat{\mathcal{H}}$, i.e. $\hat{\mathcal{H}}|\psi\rangle = E|\psi\rangle$. With this objective in mind, we act $\hat{\mathcal{H}}$ on two spin operators,

$$\hat{\mathcal{H}}\hat{S}^+_i\hat{S}^+_j|F\rangle = \left[E_F\hat{S}^+_i\hat{S}^+_j + 2JS\hat{S}^+_i\sum_\tau(\hat{S}^+_{j+\tau} - \hat{S}^+_j) + 2JS\hat{S}^+_j\sum_\tau(\hat{S}^+_{i+\tau} - \hat{S}^+_i) + 2J\hat{S}^+_i\hat{S}^+_j\delta_{\langle i,j\rangle} - \delta_{ij}\hat{S}^+_i\sum_\tau\hat{S}^+_{i+\tau}\right]|F\rangle, \tag{S14}$$

where $\sum_\tau$ denotes summation over nearest neighbors. Projecting the results on $\langle F|\hat{S}_l^- \hat{S}_m^-$ gives rise to the eigenvalue equations

$$2JS\sum_\tau(\psi_{l,m+\tau} - \psi_{l,m} + \psi_{l+\tau,m} - \psi_{l,m}) + \frac{J}{2}[\psi_{l,m} + \psi_{m,l} - \psi_{l,l} - \psi_{m,m}]\delta_{\langle l,m\rangle} = E\psi_{l,m}, \tag{S15}$$

valid for $m \neq l$, and

$$2JS(\psi_{l,l+1} - \psi_{l,l}) + 2JS(\psi_{l+1,l} - \psi_{l,l}) = E\psi_{l,l}, \tag{S16}$$

valid for $m = l$. In Eq.(S15), $\delta_{\langle l,m\rangle}$ is 1 if l and m are nearest neighbors and 0 otherwise, and we substracted E_F from E. Because of periodic boundary conditions, we can write $\psi_{i,j}$ in the center of mass frame as $\psi_{i,j} = \frac{e^{i\boldsymbol{K}\cdot\boldsymbol{R}}}{N}\sum_{\boldsymbol{q}}\psi_{\boldsymbol{K},\boldsymbol{q}}e^{i\boldsymbol{q}\cdot\boldsymbol{r}}$, where $\boldsymbol{K} = \boldsymbol{k} + \boldsymbol{p}$, $\boldsymbol{q} = (\boldsymbol{k} - \boldsymbol{p})/2$, $\boldsymbol{R} = (\boldsymbol{r}_i + \boldsymbol{r}_j)/2$ and $\boldsymbol{r} = \boldsymbol{r}_i - \boldsymbol{r}_j$, which gives rise to the eigenvalue equations

$$(\varepsilon_{\boldsymbol{k}} + \varepsilon_{\boldsymbol{p}} - E)\psi_{\boldsymbol{K},\boldsymbol{q}} = \frac{J}{N}\sum_{\boldsymbol{k}\tau}\cos(\boldsymbol{q}\cdot\boldsymbol{\tau})\left[\cos(\boldsymbol{K}\cdot\boldsymbol{\tau}/2) - \cos(\boldsymbol{k}\cdot\boldsymbol{\tau})\right]\psi_{\boldsymbol{K},\boldsymbol{k}}. \tag{S17}$$

This is the two-magnon eigenvalue equation in the center of mass frame. The eigenstates of Eq.(S17) can be found using the S-matrix approach. We first note that the exact eigenstates can be labeled with the momenta of the incoming magnons, $\boldsymbol{k} = \boldsymbol{K}/2 + \boldsymbol{q}_0$ and $\boldsymbol{p} = \boldsymbol{K}/2 - \boldsymbol{q}_0$. Under this picture, the matrix elements for two magnon scattering is given by

$$\langle F|\hat{S}^-_{\boldsymbol{k}+\boldsymbol{q}}\hat{S}^-_{\boldsymbol{p}-\boldsymbol{q}}|\boldsymbol{k},\boldsymbol{p}\rangle = \psi_{\boldsymbol{K},\boldsymbol{q}}, \tag{S18}$$

and 0 for momentum non-conserving processes. Singling out $\boldsymbol{q}_0$ in Eq.(S17), the eigenstate equations for the remaining $\boldsymbol{q}$ vectors is given by

$$\lambda_{\boldsymbol{q}}\psi_{\boldsymbol{q}} = \frac{J}{N}\sum_{\boldsymbol{p}}\Gamma_{\boldsymbol{q}\boldsymbol{p}}\psi_{\boldsymbol{q}} + \frac{J}{N}\Gamma_{\boldsymbol{q}\boldsymbol{q}_0}, \quad \boldsymbol{q} \neq \pm\boldsymbol{q}_0, \tag{S19}$$

where we defined the quantities

$$\lambda_{\boldsymbol{q}} = \varepsilon_{\boldsymbol{K}/2+\boldsymbol{q}} + \varepsilon_{\boldsymbol{K}/2-\boldsymbol{q}} - E, \quad \Gamma_{\boldsymbol{q}\boldsymbol{p}} = \sum_{\boldsymbol{\tau}}\cos(\boldsymbol{q}\cdot\boldsymbol{\tau})\left[\cos(\boldsymbol{K}\cdot\boldsymbol{\tau}/2) - \cos(\boldsymbol{k}\cdot\boldsymbol{\tau})\right], \tag{S20}$$

and, for compactness, we removed the subindex $\boldsymbol{K}$ from all quantities. Equation (S19) can be written more conveniently as

$$\psi_{\boldsymbol{q}} = \frac{J}{N}\frac{1}{\lambda_{\boldsymbol{q}}}(\Lambda_{\boldsymbol{q}} + \Gamma_{\boldsymbol{q}\boldsymbol{q}_0}), \tag{S21}$$

where $\Lambda_{\boldsymbol{q}} = \sum_{\boldsymbol{p}}\Gamma_{\boldsymbol{q}\boldsymbol{p}}\psi_{\boldsymbol{p}}$ satisfies the self-consistent equation

$$\Lambda_{\boldsymbol{q}} = \frac{J}{N}\sum_{\boldsymbol{p}}\left(\Gamma_{\boldsymbol{q}\boldsymbol{p}}\frac{1}{\lambda_{\boldsymbol{p}}}\Lambda_{\boldsymbol{p}} + \Gamma_{\boldsymbol{q}\boldsymbol{p}}\frac{1}{\lambda_{\boldsymbol{p}}}\Gamma_{\boldsymbol{p}\boldsymbol{q}_0}\right), \tag{S22}$$

The exact solution for $\Lambda_{\boldsymbol{k}}$ is

$$\Lambda_{\boldsymbol{q}} = \sum_{\boldsymbol{k}\boldsymbol{p}}\left(1 - \frac{J}{N}\Gamma_{\boldsymbol{k}\boldsymbol{q}}\frac{1}{\lambda_{\boldsymbol{q}}}\right)^{-1}\frac{J}{N}\Gamma_{\boldsymbol{k}\boldsymbol{p}}\frac{1}{\lambda_{\boldsymbol{p}}}\Gamma_{\boldsymbol{p}\boldsymbol{q}_0}. \tag{S23}$$

Using $\Lambda_{\boldsymbol{q}}$ into Eq.(S21) results in the wavefunction in the center of mass frame:

$$\psi_{\boldsymbol{q}} = \sum_{\boldsymbol{p}}\left(1 - \frac{J}{N}\Gamma_{\boldsymbol{p}\boldsymbol{q}}\frac{1}{\lambda_{\boldsymbol{q}}}\right)^{-1}\frac{J}{N}\frac{1}{\lambda_{\boldsymbol{q}}}\Gamma_{\boldsymbol{q}\boldsymbol{q}_0}. \tag{S24}$$

Within the Born approximation, the wavefunction can be approximated as $\psi_{\boldsymbol{q}} \approx \frac{J}{N}\frac{1}{\lambda_{\boldsymbol{q}}}\Gamma_{\boldsymbol{q}\boldsymbol{q}_0}$. Further, for small wavevectors of the incoming particles, we can approximate $\Gamma_{\boldsymbol{q}\boldsymbol{q}_0} \approx a^2(\boldsymbol{k}\cdot\boldsymbol{p})$. As a result, the exact two magnon eigenstates (at low momenta of incoming particles) can be interpreted as the scattering states of two spin waves coupled by the bare interaction of the form $\langle F|\hat{S}^-_{\boldsymbol{k}+\boldsymbol{q}}\hat{S}^-_{\boldsymbol{p}-\boldsymbol{q}}|\boldsymbol{k},\boldsymbol{p}\rangle \approx Ja^2(\boldsymbol{k}\cdot\boldsymbol{p})$.

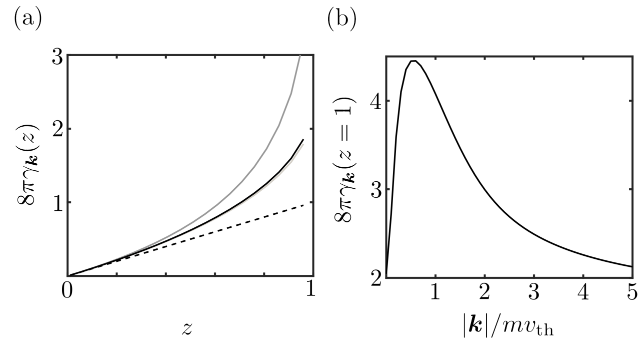

FIG. S1. (a) $\gamma_{\boldsymbol{k}}(z)$ plotted for different values $|\boldsymbol{k}|/mv_{\rm th} = 0, 1, 5$ (increasing darkness). Indicated with dashed line is the linear $\gamma_{\boldsymbol{k}}(z) \approx z/8\pi$. (b) $\gamma_{\boldsymbol{k}}(z)$ exhibits a weak dependence on k, as shown for $z = 1$. At most, $\gamma_{\boldsymbol{k}}(z)$ varies by a factor of ~ 2.5 as k is varied.

B. RELAXATION TIME DUE TO EXCHANGE COUPLING

To estimate the typical relaxation time induced by the exchange interaction, we consider a magnon fluid at thermodynamic equilibrium and zero drift velocity, $\bar{n}_{\boldsymbol{k}} = 1/(z^{-1}e^{\varepsilon_{\boldsymbol{k}}/T} - 1)$. Let us a assume that, at $t = 0$, a non-equilibrium distribution is formed with a bump at wavevector $\boldsymbol{k}$, i.e. $n_{\boldsymbol{p}} = \bar{n}_{\boldsymbol{p}} + \delta n_{\boldsymbol{k}}\delta_{\boldsymbol{k},\boldsymbol{p}}$. The relaxation time for such a distribution is given by

$$\frac{1}{\tau_{\boldsymbol{k}}} = \frac{(Ja^2)^2}{N^2}\sum_{\boldsymbol{pq}}(\boldsymbol{k}\cdot\boldsymbol{p})^2 2\pi\delta(\varepsilon_{\boldsymbol{k}} + \varepsilon_{\boldsymbol{p}} - \varepsilon_{\boldsymbol{k}+\boldsymbol{q}} - \varepsilon_{\boldsymbol{p}-\boldsymbol{q}})\left[\bar{n}_{\boldsymbol{p}}(1+\bar{n}_{\boldsymbol{k}+\boldsymbol{q}})(1+\bar{n}_{\boldsymbol{p}-\boldsymbol{q}}) - (1+\bar{n}_{\boldsymbol{p}})\bar{n}_{\boldsymbol{k}+\boldsymbol{q}}\bar{n}_{\boldsymbol{p}-\boldsymbol{q}}\right]. \tag{S25}$$

The relaxation time at wavevector $k = |\boldsymbol{k}|$ can be expressed as $\frac{1}{\tau_{\boldsymbol{k}}} = \frac{\gamma_{\boldsymbol{k}}(z)}{16\pi}\frac{T^2(ka)^2}{J}$, after pulling the $\boldsymbol{k}$ vector out of the integral, normalizing energies with T, and momenta with $\sqrt{2mT}$. The dimensionless number $\gamma_{\boldsymbol{k}}(z)$, plotted in Fig.S1, has a weak dependence on $\boldsymbol{k}$ and scales approximately as $\propto z$. Rather than keeping this uninteresting $\boldsymbol{k}$ dependence of $\gamma_{\boldsymbol{k}}$, here define an average γ of all $\boldsymbol{k}$ vectors and z values, $\gamma(z)/z = \int_0^1 dz/z \int d^2\tilde{\boldsymbol{k}}/(2\pi)^2\gamma_{\boldsymbol{k}}(z)$, which yields $\gamma(z) \approx cz$, with $c \sim 0.1$. In thermal equilibrium, the typical relaxation time for thermal magnons is given by $\bar{\tau} = \frac{8\pi}{\gamma}\frac{g_1(z)}{zg_2(z)}\frac{J^2}{T^3}$. The relaxation length of thermal magnons is given by $\xi = v_{\rm th}\bar{\tau}$, where $v_{\rm th}^2 = \frac{1}{2\pi mn}\int_0^\infty dk k^3\bar{n}_{\boldsymbol{k}} = 2mTg_2(z)/g_1(z)$ is the thermal velocity. In the limit $z \ll 1$, this gives Eq.(1) of the main text.

C. ESTIMATING TRANSPORT COEFFICIENTS FROM THE RELAXATION TIME APPROXIMATION

To compute the leading order corrections to $P_{\alpha\beta}$ and q_α beyond the local equilibrium approximation, we need to determine $\delta n_{\boldsymbol{k}}$ induced by gradients in n, u_α, and θ. With this objective in mind, we replace $n_{\boldsymbol{k}} = \bar{n}_{\boldsymbol{k}} + \delta n_{\boldsymbol{k}}$ into Boltzmann equation (6) of the main text, and keep leading order terms in $\delta n_{\boldsymbol{k}}$:

$$(\partial_t + v_{\boldsymbol{k},\alpha}\partial_\alpha + F_\alpha\partial_{k_\alpha})\,\bar{n}_{\boldsymbol{k}} = \mathcal{I}(\bar{n}_{\boldsymbol{k}} + \delta n_{\boldsymbol{k}}). \tag{S26}$$

Here we assumed that $\delta n_{\boldsymbol{k}} \ll \bar{n}_{\boldsymbol{k}}$, such that the leading order contributions on the left-hand is given by the derivatives (both space and time) of $\bar{n}_{\boldsymbol{k}}$. The right-hand side is already leading order in $\delta n_{\boldsymbol{k}}$ because $\mathcal{I}(\bar{n}_{\boldsymbol{k}}) = 0$ by definition of $\bar{n}_{\boldsymbol{k}}$.

We begin the analysis by considering the left-hand side of Eq.(S26). We recall that $\bar{n}_{\boldsymbol{k}}(n, u_\alpha, \theta)$ is the local distribution function which depends implicitly on n, u_α and θ via Eq.(10) of the main text. As such, computing the time and spatial derivatives of $\bar{n}_{\boldsymbol{k}}$ leads to

$$\left[\partial_t + v_{\boldsymbol{k},\alpha}\partial_\alpha\right]\bar{n}_{\boldsymbol{k}} = \left[\dot{n} + v_{\boldsymbol{k},\alpha}\partial_\alpha n\right]\partial_n\bar{n}_{\boldsymbol{k}}\big|_{\theta,u_\alpha} + \left[\dot{\theta} + v_{\boldsymbol{k},\alpha}\partial_\alpha\theta\right]\partial_\theta\bar{n}_{\boldsymbol{k}}\big|_{n,u_\alpha} + \left[\dot{u}_\alpha + v_{\boldsymbol{k},\beta}\partial_\beta u_\alpha\right]\partial_{u_\alpha}\bar{n}_{\boldsymbol{k}}\big|_{n,\theta}, \tag{S27}$$

where we denote $\partial\bar{n}_{\boldsymbol{k}}/\partial x|_{y,z}$ as the derivative of $\bar{n}_{\boldsymbol{k}}$ with respect to x, leaving y and z constant. In Eq.(S28), we replace the time derivatives $\dot{n}$, $\dot{u}_\alpha$, and $\dot{\theta}$ by the hydrodynamic equations (12) of the main text in the local equilibrium approximation, i.e. using $P_{\alpha\beta} = \delta_{\alpha\beta}n\theta/m$ and $q_\alpha = 0$, and use the identity $\partial\bar{n}_{\boldsymbol{k}}/\partial u_\alpha|_{n,\theta} = -[\partial\bar{n}_{\boldsymbol{k}}/\partial\theta_{\boldsymbol{k}}]m\tilde{v}_{\boldsymbol{k},\alpha}$. This results in

$$[\partial_t + v_{\boldsymbol{k},\alpha}\partial_\alpha + F_\alpha \partial_{k_\alpha}]\,\bar{n}_{\boldsymbol{k}} = \left[\delta_{\alpha\beta}\partial_n \bar{n}_{\boldsymbol{k}}\big|_{\theta,u_\alpha} + \frac{m}{n}\partial_n P_{\alpha\beta}\partial_{\theta_{\boldsymbol{k}}}\bar{n}_{\boldsymbol{k}}\right]\tilde{v}_{\boldsymbol{k},\beta}\partial_\alpha n + \left[\delta_{\alpha\beta}\partial_\theta \bar{n}_{\boldsymbol{k}}\big|_{n,u_\alpha} + \frac{m}{n}\partial_\theta P_{\alpha\beta}\partial_{\theta_{\boldsymbol{k}}}\bar{n}_{\boldsymbol{k}}\right]\tilde{v}_{\boldsymbol{k},\beta}\partial_\alpha \theta$$
$$- \left[\delta_{\alpha\beta} n\partial_n \bar{n}_{\boldsymbol{k}}\big|_{\theta,u_\alpha} + \frac{m}{n}P_{\alpha\beta}\partial_\theta \bar{n}_{\boldsymbol{k}}\big|_{n,u_\alpha} + m\tilde{v}_{\boldsymbol{k},\alpha}\tilde{v}_{\boldsymbol{k},\beta}\partial_{\theta_{\boldsymbol{k}}}\bar{n}_{\boldsymbol{k}}\right]\partial_\alpha u_\beta, \tag{S28}$$

where we used $F_\alpha \partial_{k_\alpha}\bar{n}_{\boldsymbol{k}} = F_\alpha[\partial\bar{n}_{\boldsymbol{k}}/\partial\theta_{\boldsymbol{k}}]\tilde{v}_{\boldsymbol{k},\alpha}$. The terms in brackets in Eq.(S28) are thermodynamic functions that depend on the local values of (T, z, w_α), and are given by

$$[\partial_t + v_{\boldsymbol{k},\alpha}\partial_\alpha + F_\alpha \partial_{k_\alpha}]\,\bar{n}_{\boldsymbol{k}} = \left[\frac{2\pi}{mT}\left(h_n(z) + \tilde{h}_n(z)\frac{\theta_{\boldsymbol{k}}}{T}\right)\tilde{v}_{\boldsymbol{k},\alpha}\partial_\alpha n + \frac{2\pi}{T}\left(h_\theta(z) + \tilde{h}_\theta(z)\frac{\theta_{\boldsymbol{k}}}{T}\right)\tilde{v}_{\boldsymbol{k},\alpha}\partial_\alpha\theta \right.$$
$$\left. + \left(\delta_{\alpha\beta}\frac{\theta_{\boldsymbol{k}}}{T} - \frac{m v_{\boldsymbol{k},\alpha} v_{\boldsymbol{k},\beta}}{T}\right)\partial_\alpha u_\beta\right]\bar{n}_{\boldsymbol{k}}(\bar{n}_{\boldsymbol{k}}+1), \tag{S29}$$

where the dimensionless coefficients $h_{n,\theta}(z)$ and $\tilde{h}_{n,\theta}(z)$ are given by

$$h_n(z) = \frac{zg_2^2 - (1-z)g_2 g_1^2}{zg_2 g_1^2 - (1-z)g_1^4/2}, \quad \tilde{h}_n(z) = \left[\frac{1}{g_1} + \frac{zg_2}{g_1^2(1-z) - 2zg_2}\right],$$
$$h_\theta(z) = \frac{zg_2^2 - (1-z)g_2 g_1^2}{zg_2 g_1^2 - (1-z)g_1^4/2}, \quad \tilde{h}_\theta(z) = \left[\frac{1}{g_1} + \frac{zg_2}{g_1^2(1-z) - 2zg_2}\right]. \tag{S30}$$

Let us now turn to the right-hand side of Eq.(S26). There are many schemes to calculate $\mathcal{I}[\bar{n}_{\boldsymbol{k}} + \delta n_{\boldsymbol{k}}]$. The simplest approach is to use the *relaxation time approximation.* In this approximation, the collision integral is written as $\mathcal{I}[\bar{n}_{\boldsymbol{k}} + \delta n_{\boldsymbol{k}}] \approx -\delta n_{\boldsymbol{k}}/\tau_{\boldsymbol{k}}$, where $\tau_{\boldsymbol{k}}$ is defined in Eq.(S46). Importantly, we keep the explicit dependence magnon wavevector. We note that Eq.(S46) was calculated using $u_\alpha = 0$, and remains to be valid in the regime $u_\alpha \lesssim \sqrt{T/m}$ [corrections to $1/\tau_{\boldsymbol{k}}$ due to finite drift velocity are $\mathcal{O}(u_\alpha^2)$]. As a result, $\delta f_{\boldsymbol{k}}$ becomes proportional to gradients in n, θ, and u_α:

$$\delta n_{\boldsymbol{k}} = \tau_{\boldsymbol{k}}\left[\frac{2\pi}{mT}\left(h_n(z) + \tilde{h}_n(z)\frac{\theta_{\boldsymbol{k}}}{T}\right)\tilde{v}_{\boldsymbol{k},\alpha}\partial_\alpha n + \frac{2\pi}{T}\left(h_\theta(z) + \tilde{h}_\theta(z)\frac{\theta_{\boldsymbol{k}}}{T}\right)\tilde{v}_{\boldsymbol{k},\alpha}\partial_\alpha\theta \right.$$
$$\left. + \left(\delta_{\alpha\beta}\frac{\theta_{\boldsymbol{k}}}{T} - \frac{m v_{\boldsymbol{k},\alpha} v_{\boldsymbol{k},\beta}}{T}\right)\partial_\alpha u_\beta\right]\bar{n}_{\boldsymbol{k}}(\bar{n}_{\boldsymbol{k}}+1). \tag{S31}$$

Using $n_{\boldsymbol{k}} = \bar{n}_{\boldsymbol{k}} + \delta n_{\boldsymbol{k}}$ in Eq.(11) of the main text, and integrating over $\boldsymbol{k}$ leads to

$$P_{\alpha\beta} = \frac{n\theta}{m}\delta_{\alpha\beta} + \mu\left(\partial_\alpha u_\beta + \partial_\beta u_\alpha\right) - \mu\delta_{\alpha\beta}\partial_\gamma u_\gamma, \quad q_\alpha = \kappa_n \partial_\alpha n + \kappa_\theta \partial_\alpha \theta, \tag{S32}$$

where only linear terms on $\partial_\alpha n$, $\partial_\alpha\theta$, and $\partial_\alpha u_\beta$ were considered (i.e., gradients of thermodynamic quantities are small). For a two-dimensional magnon gas with quadratic dispersion and collision rate of the form $1/\tau_{\boldsymbol{k}} \propto \boldsymbol{k}^2$ (i.e., only considering exchange coupling), the relaxation time yields that dissipation is dominated by viscocity $\mu(T,z) = \frac{\pi}{2}\frac{J^2 g_1(z)}{T\bar{\gamma}(z)}$, while $\kappa_n = \kappa_\theta$ are second order effects compared to μ. In particular, κ_n and κ_θ are dominated by deviations to quadratic dispersion and/or finite scattering at low scattering, e.g. dipolar interactions.

D. TRANSVERSE SPIN FLUCTUATIONS

The spectral weight of the correlator $\chi_{+-}(\boldsymbol{k},\omega) = -i\int_0^\infty dt e^{i\omega t}\langle[\hat{S}^-_{-\boldsymbol{k}}, S^+_{\boldsymbol{k}}(0)]\rangle$ is concentrated at the magnon frequency $\omega_{\boldsymbol{k}} = \Delta + \varepsilon_{\boldsymbol{k}}$ and is associated to the production of a single magnon. Off-resonant processes, however, give rise to a finite contribution to $\chi_{-+}(\boldsymbol{k},\omega)$ even below the magnon gap, see Fig.S2(a). As such, we estimate the contribution of such processes in the noise spectrum and show that they give a small contribution to χ_{+-} compare to that of the sound mode. With this objective in mind, we calculate the leading order contribution of the imaginary part of the magnon self-energy $\Sigma(\boldsymbol{k},\omega)$, and approximate the correlation function as

$$\chi_{+-}(\boldsymbol{k},\omega) = \frac{1}{\omega - \omega_{\boldsymbol{k}} + i\Sigma''(\boldsymbol{k},\omega)}, \tag{S33}$$

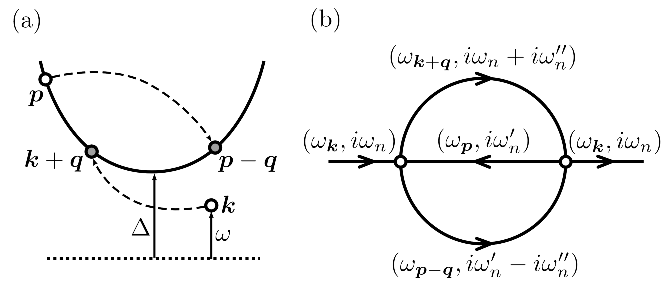

FIG. S2. (a) In addition to the sound mode, off-resonant processes can also give a finite contribution to χ_{-+} below the magnon gap. (b) Sunrise diagram contributing to the magnon self-energy of χ_{-+}.

where energy shifts to the single magnon dispersion are neglected. From the effective interaction in Eq.(5) of the main text, this is given by the second order process depicted in Fig.S2(b). In terms of Matsubara frequencies, it can be written as

$$\Sigma(\boldsymbol{k},\omega) = -J^2a^4 \sum_{\boldsymbol{pq}} \sum_{i\omega'_n i\omega''_n} (\boldsymbol{k}\cdot\boldsymbol{p})^2 \frac{1}{(i\omega'_n - \omega_{\boldsymbol{p}})(i\omega_n + i\omega''_n - \omega_{\boldsymbol{k}+\boldsymbol{q}})(i\omega'_n - i\omega''_n - \omega_{\boldsymbol{p}-\boldsymbol{q}})}. \tag{S34}$$

The retarded correlator is obtained by analytical continuatio $i\omega_n \to \omega + i\epsilon$ and taking the imaginary part of the resulting expression:

$$\Sigma''(\boldsymbol{k},\omega) = J^2a^4 \sum_{\boldsymbol{pq}} (\boldsymbol{k}\cdot\boldsymbol{p})^2 \delta(\omega - \Delta + \varepsilon_{\boldsymbol{p}} - \varepsilon_{\boldsymbol{k}+\boldsymbol{q}} - \varepsilon_{\boldsymbol{p}-\boldsymbol{q}})(n_{\boldsymbol{p}} - \tilde{n}_{\boldsymbol{p}})(1 + n_{\boldsymbol{k}+\boldsymbol{q}} + n_{\boldsymbol{p}-\boldsymbol{q}}), \tag{S35}$$

where we denote $\tilde{n}_{\boldsymbol{p}} = n(\varepsilon_{\boldsymbol{k}} + \omega)$. A similar analysis follows for the correlator $\chi_{+-}(\omega) \approx \delta(\omega + \omega_{\boldsymbol{k}})$. Dimensional analysis in the limit $\omega \ll T$ yields Σ'' scaling as $\Sigma(\boldsymbol{k},\omega) = \frac{T\omega}{J}(ka)^2$.

E. MEASUREMENT OF MAGNON SOUND MODES

We consider a spin-1/2 qubit with an intrinsic level splitting ω_{q} placed a distance d above the magnetic insulator. The dynamics of the qubit and the ferromagnet is governed by the Hamiltonian $\hat{\mathcal{H}} = \hat{\mathcal{H}}_{\mathrm{F}} + \hat{\mathcal{H}}_{\mathrm{F-q}} + \hat{\mathcal{H}}_{\mathrm{q}}$. Here $\mathcal{H}_{\mathrm{F}}$ is the Hamiltonian of the ferromagnet, see main text. The term $\hat{\mathcal{H}}_{\mathrm{q}}$ is the qubit Hamiltonian given by $\hat{\mathcal{H}}_{\mathrm{q}} = \frac{1}{2}\omega \boldsymbol{n}_{\mathrm{q}} \cdot \boldsymbol{\sigma}$, where $\boldsymbol{n}_{\mathrm{q}}$ is the intrinsic polarizing field of the spin probe. For instance, in the case of NV centers in diamons, $\boldsymbol{n_q}$ is the axis of the NV defect in the diamond lattice. Finally, the term $\hat{\mathcal{H}}_{\mathrm{F-q}}$ is the qubit-ferromagnet coupling, given by

$$\mathcal{H}_{\mathrm{F-q}} = \frac{\mu_{\mathrm{B}}^2}{2} \hat{\boldsymbol{\sigma}} \cdot \hat{\boldsymbol{B}}, \quad \hat{\boldsymbol{B}} = \frac{1}{4\pi} \sum_j \left[\frac{\hat{\boldsymbol{S}}_j}{r_j^3} - \frac{3(\hat{\boldsymbol{S}}_j \cdot \boldsymbol{r}_j)\boldsymbol{r}_j}{r_j^5} \right], \tag{S36}$$

where $\boldsymbol{B}$ is the magnetic field at the position of the probe induced by dipolar interactions with the 2D ferromagnet, and $\boldsymbol{r}_j = (x_j, y_j, -d)$ is the relative position between the i-th spin in the 2D lattice and probe.

In thermal equilibrium, the 2D ferromagnet is described by the density matrix $\rho_{\mathrm{F}} = \sum_n e^{-\varepsilon_n/k_{\mathrm{B}}T} |n\rangle\langle n|$, where $|n\rangle$ are the eigenstates of the ferromagnet. The absorption rate, $1/T_{1,\mathrm{abs}}$, and emission rate, $1/T_{1,\mathrm{em}}$, is obtained from Fermi Golden's rule using the initial state $|i\rangle = |-\rangle \otimes \rho_{\mathrm{F}}$ and $|i\rangle = |+\rangle \otimes \rho_{\mathrm{F}}$, respectively:

$$1/T_{\mathrm{abs,em}} = 2\pi \sum_{nm} \rho_n B^{\pm}_{nm} B^{\mp}_{mn} \delta(\omega \pm \varepsilon_{mn}). \tag{S37}$$

Here B^{α}_{nm} denotes $\langle n|\hat{B}^{\alpha}|m\rangle$, and ε_{mn} is the energy difference between states m and n, $\varepsilon_{mn} = \varepsilon_m - \varepsilon_n$. The relaxation rate is defined as $1/T_1 = \frac{1}{2}[1/T_{\mathrm{abs}} + T_{\mathrm{em}}]$. More compactly, $1/T_1$ can be expressed as

$$\frac{1}{T_1} = \frac{\mu_{\mathrm{B}}^2}{2} \int_{-\infty}^{\infty} dt e^{i\omega t} \langle \{\hat{B}^-(t), \hat{B}^+(0)\}\rangle. \tag{S38}$$

For computation it is more convenient to express $1/T_1$ in terms of retarded correlation functions. In this direction, the fluctuation-dissipation theorem reads

$$\int_{-\infty}^{\infty} dt e^{i\omega t} \langle \{\hat{B}^-(t), \hat{B}^+(0)\}\rangle = \coth\left(\frac{\omega}{2T}\right) \mathrm{Im}\left[\chi^{\mathrm{R}}_{B^-B^+}(\omega)\right], \tag{S39}$$

where $\chi^{\mathrm{R}}_{B^-B^+}(\omega) = -i\int_0^\infty dt \langle [\hat{B}^-(t), \hat{B}^+(0)] \rangle$ is the retarded correlation function.

Finally, $1/T_1$ can be expressed in terms of spin-spin correlation functions. Expressing $\hat{S}^\alpha_\tau = \sum_{\boldsymbol{k}} \frac{e^{i\boldsymbol{k}\cdot\boldsymbol{\tau}}}{\sqrt{N}} \hat{S}^\alpha_{\boldsymbol{k}}$ in momentum space and inserting into Eq.(S36), we can express $\hat{B}^\alpha$ in terms of $S^\pm_{\boldsymbol{k}}$ and $S^z_{\boldsymbol{k}}$. Without loss of generality, we assume $\boldsymbol{k} = (k, 0)$. For $\hat{B}^x$, we find

$$\hat{B}^x_{\boldsymbol{k}} = \sum_j e^{ikx_j} \left[\left(\frac{1}{r_j^3} - \frac{3x_j^2}{r_j^5} \right) S^x_{\boldsymbol{k}} - \frac{3x_j y_j}{r_j^5} S^y_{\boldsymbol{k}} + \frac{3x_j d}{r_j^5} S^z_{\boldsymbol{k}} \right]. \tag{S40}$$

Using the continuum approximation to approximate $\sum_j \to \frac{1}{a^2}\int d^2\boldsymbol{x}$, the first term on the right-hand side of Eq.(S40) is

$$\sum_j e^{ikx_j} \left(\frac{1}{r_j^3} - \frac{3x_j^2}{r_j^5} \right) \to \frac{1}{a^2} \iint dxdy\, e^{ikx} \left(\frac{1}{r^3} - \frac{3x^2}{r^5} \right) = \frac{2}{a^2} \int dx e^{ikx} \frac{d^2 - x^2}{(d^2+x^2)^2} = \frac{2}{da^2} \int d\xi e^{i(kd)\xi} \frac{1-\xi^2}{(1+\xi^2)^2}. \tag{S41}$$

In the last step, we can use the residue theorem to express $\int_{-\infty}^\infty d\xi e^{i(kd)\xi} \frac{1-\xi^2}{(1+\xi^2)^2}$ as $\oint dz e^{i(kd)z} \frac{1-z^2}{(1+z^2)^2} = \pi(kd)e^{-kd}$, where for $kd > 0$ we use a contour of integration in the upper-half complex plane. As a result, we obtain

$$\sum_j e^{ikx_j} \left(\frac{1}{r_j^3} - \frac{3x_j^2}{r_j^5} \right) \approx \frac{ke^{-kd}}{2a^2}, \tag{S42}$$

exact in the continuum limit. For the second term on the right-hand side of Eq.(S40), we find $\sum_j e^{ikx_j} \frac{x_j y_j}{r_j^5} = 0$. Finally, for the third term in the right-hand side of Eq.(S40), we find

$$3\sum_j e^{ikx_j} \frac{x_j d}{r_j^5} \approx \frac{3ikd}{a^2} \iint dx\, dy \frac{x^2}{r^5} = \frac{ik}{2a^2}. \tag{S43}$$

Repeating the same procedure for $\hat{B}^y$ and $\hat{B}^z$, and generalizing our results for a generic $\boldsymbol{k} = (k_x, k_y)$, we obtain $\hat{B}^\alpha = \frac{1}{\sqrt{N}} \sum_{\boldsymbol{k}} B^\alpha_{\boldsymbol{k}}$, with

$$\begin{pmatrix} \hat{B}^x_{\boldsymbol{k}} \\ \hat{B}^y_{\boldsymbol{k}} \\ \hat{B}^z_{\boldsymbol{k}} \end{pmatrix} = \frac{e^{-|\boldsymbol{k}|z}}{2a^2} \begin{pmatrix} k_x^2/|\boldsymbol{k}| & k_x k_y/|\boldsymbol{k}| & ik_x \\ k_x k_y/|\boldsymbol{k}| & k_y^2/|\boldsymbol{k}| & ik_y \\ ik_x & ik_y & -|\boldsymbol{k}| \end{pmatrix} \begin{pmatrix} \hat{S}^x_{\boldsymbol{k}} \\ \hat{S}^y_{\boldsymbol{k}} \\ \hat{S}^z_{\boldsymbol{k}} \end{pmatrix}. \tag{S44}$$

The $B^\pm_{\boldsymbol{k}} = B^x_{\boldsymbol{k}} \pm iB^y_{\boldsymbol{k}}$ terms can be written as a function of $S^\pm_{\boldsymbol{k}}$ and $S^z_{\boldsymbol{k}}$ such that Eq.(S44) can be recasted as

$$\begin{pmatrix} \hat{B}^+_{\boldsymbol{k}} \\ \hat{B}^-_{\boldsymbol{k}} \\ \hat{B}^z_{\boldsymbol{k}} \end{pmatrix} = \frac{e^{-|\boldsymbol{k}|z}}{2a^2} \begin{pmatrix} |\boldsymbol{k}|/2 & (k_x+ik_y)^2/2|\boldsymbol{k}| & ik_x - k_y \\ (k_x-ik_y)^2/2|\boldsymbol{k}| & |\boldsymbol{k}|/2 & ik_x + k_y \\ (ik_x+k_y)/2 & (ik_x-k_y)/2 & -|\boldsymbol{k}| \end{pmatrix} \begin{pmatrix} \hat{S}^+_{\boldsymbol{k}} \\ \hat{S}^-_{\boldsymbol{k}} \\ \hat{S}^z_{\boldsymbol{k}} \end{pmatrix}. \tag{S45}$$

Using Eq.(S45) in Eq.(S38), the spin qubit relaxation time is given by

$$\frac{1}{T_1} = \coth\left(\frac{\omega}{2T}\right) \frac{\mu_{\mathrm{B}}^2}{2a^2} \int \frac{d^2\boldsymbol{k}}{(2\pi)^2} e^{-2|\boldsymbol{k}|d} |\boldsymbol{k}|^2 \left[\chi^{\mathrm{R}}_{-+}(\boldsymbol{k},\omega) + \chi^{\mathrm{R}}_{+-}(\boldsymbol{k},\omega) + 4\chi^{\mathrm{R}}_{zz}(\boldsymbol{k},\omega) \right], \tag{S46}$$

where we denote $\chi^{\mathrm{R}}_{\alpha\beta}(\boldsymbol{k},\omega) = -i\int_0^\infty dt \langle [\hat{S}^\alpha_{-\boldsymbol{k}}(t), \hat{S}^\beta_{\boldsymbol{k}}(0)] \rangle$.

F. EFFECT OF DIPOLAR INTERACTIONS

Dipolar interactions, which can be sizable in a two-dimensional ferromagnet, introduce a variety of effects that need to be carefully taken into account. For instance, they add a gap to the excitation spectrum, modify the collision term by adding hard-core repulsion, and induce magnon leakage via three body interactions. We incorporate dipolar interactions via the term

$$\hat{\mathcal{H}}_{\mathrm{d}} = \frac{\mu_{\mathrm{B}}^2}{4\pi} \frac{1}{2} \sum_{jj'} \left[\frac{\hat{\boldsymbol{S}}_j \cdot \hat{\boldsymbol{S}}_{j'}}{r_{jj'}^3} - 3\frac{(\hat{\boldsymbol{S}}_j \cdot \boldsymbol{r}_{jj'})(\hat{\boldsymbol{S}}_{j'} \cdot \boldsymbol{r}_{jj'})}{r_{jj'}^5} \right], \tag{S47}$$

where $\mu_{\rm B}$ is the Bohr magneton, and $\boldsymbol{r}_{jj'}$ is the relative distance between spins j and j'. It is important to conside the combined effect of the Zeeman term,

$$\hat{\mathcal{H}}_{\rm z} = \Delta \sum_i \hat{S}^z_i, \tag{S48}$$

and dipolar interactions. In particular, in the presence of a Zeeman field, it is convenient to pick a quantization axis which is canted from the 2D plane $\boldsymbol{r} = (x, y, 0)$,

$$\hat{S}^z_j \to \cos\theta \hat{S}^z_j - \sin\theta \hat{S}^x_j, \quad \hat{S}^x_j \to \cos\theta \hat{S}^x_j + \sin\theta \hat{S}^z_j, \quad \hat{S}^y_j \to \hat{S}^y_j, \tag{S49}$$

where θ will be conveniently chosed below. Inserting Eq. (S49) into Eq. (S47), we find

$$\begin{aligned}\hat{\mathcal{H}}_{\rm d} = \frac{\mu_{\rm B}^2}{8\pi} \sum_{j\tau} \frac{1}{\tau^3} \Bigg[& \hat{S}^x_j \hat{S}^x_{j+\tau} \left(1 - 3\cos^2\theta \frac{\tau_x^2}{\tau^2}\right) + \hat{S}^y_j \hat{S}^y_{j+\tau} \left(1 - 3\frac{\tau_y^2}{\tau^2}\right) + \hat{S}^z_j \hat{S}^z_{j+\tau} \left(1 - 3\sin^2\theta \frac{\tau_x^2}{\tau^2}\right) \\ & -6\sin\theta\cos\theta \frac{\tau_x^2}{\tau^2} \hat{S}^x_j \hat{S}^z_{j+\tau} - 6\cos\theta \frac{\tau_x\tau_y}{\tau^2} \hat{S}^x_j \hat{S}^y_{j+\tau} - 6\sin\theta \frac{\tau_x\tau_y}{\tau^2} \hat{S}^z_j \hat{S}^y_{j+\tau} \Bigg],\end{aligned} \tag{S50}$$

where τ denotes relative positions between spins on a two-dimensional square lattice (not restricted to nearest neighbors). After rearranging terms, we find

$$\begin{aligned}\hat{\mathcal{H}}_{\rm d} = \frac{3\mu_{\rm B}^2}{8\pi} \sum_{j\tau} \frac{1}{\tau^3} \Bigg[& \left(\hat{\boldsymbol{S}}_j \cdot \hat{\boldsymbol{S}}_{j+\tau}\right) \left(\frac{1}{3} - \frac{\tau_x^2}{\tau^2}\right) + \sin^2\theta \frac{\tau_x^2}{\tau^2} \hat{S}^x_j \hat{S}^x_{j+\tau} + \cos^2\theta \frac{\tau_x^2}{\tau^2} \hat{S}^z_j \hat{S}^z_{j+\tau} - \frac{\tau_y^2 - \tau_x^2}{\tau^5} \hat{S}^y_j \hat{S}^y_{j+\tau} \\ & -2\sin\theta\cos\theta \frac{\tau_x^2}{\tau^2} \hat{S}^x_j \hat{S}^z_{j+\tau} - 2\cos\theta \frac{\tau_x\tau_y}{\tau^2} \hat{S}^x_j \hat{S}^y_{j+\tau} - 2\sin\theta \frac{\tau_x\tau_y}{\tau^2} \hat{S}^z_j \hat{S}^y_{j+\tau} \Bigg].\end{aligned} \tag{S51}$$

Note that the first term on the right-hand side can be incorporated into the definition of J with a small anisotropy in the x direction which we will neglect. For convenience, we define $\hat{\mathcal{H}}_{\rm d} = \hat{\mathcal{H}}_{zz} + \hat{\mathcal{H}}_{xz} + \hat{\mathcal{H}}_{xx} + \hat{\mathcal{H}}_{yy} + \hat{\mathcal{H}}_{xy} + \hat{\mathcal{H}}_{yz}$, with

$$\begin{aligned}&\hat{\mathcal{H}}_{zz} = \varepsilon_{\rm d} \cos^2\theta \frac{a^3}{\pi S^2} \sum_{j\tau} \frac{\tau_x^2}{\tau^5} \hat{S}^z_j \hat{S}^z_{j+\tau}, \ \hat{\mathcal{H}}_{xx} = \varepsilon_{\rm d} \sin^2\theta \frac{a^3}{\pi S^2} \sum_{j\tau} \frac{\tau_x^2}{\tau^5} \hat{S}^x_j \hat{S}^x_{j+\tau}, \ \hat{\mathcal{H}}_{xz} = -2\varepsilon_{\rm d} \sin\theta\cos\theta \frac{a^3}{\pi S^2} \sum_{j\tau} \frac{\tau_x\tau_y}{\tau^5} \hat{S}^x_j \hat{S}^z_{j+\tau}, \\ &\hat{\mathcal{H}}_{yy} = \varepsilon_{\rm d} \frac{a^3}{\pi S^2} \sum_{j\tau} \frac{\tau_y^2 - \tau_x^2}{\tau^5} \hat{S}^y_j \hat{S}^y_{j+\tau}, \ \hat{\mathcal{H}}_{xy} = -2\varepsilon_{\rm d} \cos\theta \frac{a^3}{\pi S^2} \sum_{j\tau} \frac{\tau_x\tau_y}{\tau^5} \hat{S}^x_j \hat{S}^y_{j+\tau}, \quad \hat{\mathcal{H}}_{yz} = -2\varepsilon_{\rm d} \sin\theta \frac{a^3}{\pi S^2} \sum_{j\tau} \frac{\tau_x\tau_y}{\tau^5} \hat{S}^y_j \hat{S}^z_{j+\tau},\end{aligned} \tag{S52}$$

where we defined the dipolar energy as

$$\varepsilon_{\rm d} = \frac{3S^2\mu_{\rm B}^2}{4a^3}. \tag{S53}$$

The Zeeman splitting term in the rotated frame is given $\hat{\mathcal{H}}_{\rm z} = \hat{\mathcal{H}}_x + \hat{\mathcal{H}}_z$ given by

$$\hat{\mathcal{H}}_x = \Delta\cos\theta \sum_j \hat{S}^x_j, \quad \hat{\mathcal{H}}_z = -\Delta\sin\theta \sum_j \hat{S}^z_j. \tag{S54}$$

Focusing on $\hat{\mathcal{H}}_{zz}$ first, we define $\hat{S}^z_j = -S(1 - \hat{n}_j)$, which leads to

$$\hat{\mathcal{H}}_{zz} = \varepsilon_{\rm d} \cos^2\theta \frac{a^3}{\pi} \sum_{j\tau} \frac{\tau_x^2}{\tau^5} (1 - 2\hat{n}_j + \hat{n}_j \hat{n}_{j+\tau}) = \varepsilon_{\rm d} \cos^2\theta \left(NS - 2\sum_j \hat{n}_j + \frac{a^3}{\pi} \sum_{j\tau} \frac{\tau_x^2}{\tau^5} \hat{n}_j \hat{n}_{j+\tau} \right), \tag{S55}$$

and where, in the last step, we used

$$\sum_{\boldsymbol{\tau}} e^{-i\boldsymbol{k}\cdot\boldsymbol{\tau}} \frac{\tau_x^2}{\tau^5} = \frac{\pi}{a^3} + \mathcal{O}(q^2). \tag{S56}$$

Similarly, for $\hat{\mathcal{H}}_{xz}$ we find

$$\hat{\mathcal{H}}_{xz} = 2\varepsilon_{\rm d}\sin\theta\cos\theta\frac{a^3}{\pi S}\sum_{j\tau}\frac{\tau_x^2}{\tau^5}\hat{S}_j^x(1-\hat{n}_{j+\tau}) = \frac{2\varepsilon_{\rm d}\sin\theta\cos\theta}{S}\left(\sum_j \hat{S}_j^x - \frac{a^3}{\pi}\sum_{j\tau}\frac{\tau_x^2}{\tau^5}\hat{S}_j^x\hat{n}_{j+\tau}\right). \tag{S57}$$

Turning to $\hat{\mathcal{H}}_{xx}$ and using $\hat{S}_j^x = (\hat{S}_j^+ + \hat{S}_j^-)/2$, we find

$$\hat{\mathcal{H}}_{xx} = \frac{\varepsilon_{\rm d}\sin^2\theta}{4}\frac{a^3}{\pi S^2}\sum_{j\tau}\frac{\tau_x^2}{\tau^5}\left(\hat{S}_j^+\hat{S}_{j+\tau}^+ + \hat{S}_j^-\hat{S}_{j+\tau}^- + 2\hat{S}_j^+\hat{S}_{j+\tau}^-\right) = \frac{\varepsilon_{\rm d}\sin^2\theta}{4S^2}\sum_{\boldsymbol{k}}\left(\hat{S}_{-\boldsymbol{k}}^+\hat{S}_{\boldsymbol{k}}^+ + \hat{S}_{-\boldsymbol{k}}^-\hat{S}_{\boldsymbol{k}}^- + 2\hat{S}_{-\boldsymbol{k}}^+\hat{S}_{\boldsymbol{k}}^-\right), \tag{S58}$$

where, in the last step, we used Eq.(S56). The term $\hat{\mathcal{H}}_{xx}$ introduces coherent creation/destruction of two magnons. The term $\hat{\mathcal{H}}_{xy}$ also introduces similar two-magnon processes as those in $\hat{\mathcal{H}}_{xx}$,

$$\hat{\mathcal{H}}_{xy} = -\frac{\varepsilon_{\rm d}\cos\theta}{2i}\frac{a^3}{\pi S^2}\sum_{j\tau}\frac{\tau_x\tau_y}{|\boldsymbol{\tau}|^5}\left(\hat{S}_j^+\hat{S}_{j+\tau}^+ - \hat{S}_j^-\hat{S}_{j+\tau}^-\right) = -\frac{2\varepsilon_{\rm d}\cos\theta}{i\pi S^2}\sum_{\boldsymbol{k}}\frac{k_xk_y}{a}\left(\hat{S}_{-\boldsymbol{k}}^+\hat{S}_{\boldsymbol{k}}^+ - \hat{S}_{-\boldsymbol{k}}^-\hat{S}_{\boldsymbol{k}}^-\right), \tag{S59}$$

but the matrix elements of $\hat{\mathcal{H}}_{xy}$ are $\mathcal{O}(q^2)$ smaller than those corresponding to $\hat{\mathcal{H}}_{xx}$ [in the last step of Eq.(S59), we used $\sum_{\boldsymbol{\tau}} e^{i\boldsymbol{k}\cdot\boldsymbol{\tau}}\frac{\tau_x\tau_y}{\tau^5} = \frac{4k_xk_y}{a} + \mathcal{O}(k^4)$]. As a result, we neglect $\hat{\mathcal{H}}_{xy}$. Finally, for $\hat{\mathcal{H}}_{yz}$, we find

$$\begin{aligned}\hat{\mathcal{H}}_{yz} &= -2\varepsilon_{\rm d}\sin\theta\frac{a^3}{\pi S}\sum_{j\tau}\frac{\tau_x\tau_y}{\tau^5}\hat{S}_j^y(1-n_{j+\tau}) = -2\varepsilon_{\rm d}\sin\theta\frac{a^3}{\pi S}\left(\sum_{j\tau}\frac{\tau_x\tau_y}{\tau^5}\hat{S}_j^y - \sum_{j\tau}\frac{\tau_x\tau_y}{\tau^5}\hat{S}_j^y\hat{n}_{j+\tau}\right)\\ &= 6\varepsilon_{\rm d}\sin\theta\frac{a^3}{\pi S}\sum_{j\tau}\frac{\tau_x\tau_y}{\tau^5}\hat{S}_j^y\hat{n}_{j+\tau},\end{aligned} \tag{S60}$$

where the first term in the third equality is zero because $\sum_{\boldsymbol{\tau}}\tau_x\tau_y/\tau^5 = 0$, thus giving only a cubic term. The cubic term, however, has matrix elements $\mathcal{O}(q^2)$ smaller than those corresponing to $\hat{\mathcal{H}}_{xz}$ because of the factors $\tau_x\tau_y$. As a result, we neglect the matrix elements introduced by $\hat{\mathcal{H}}_{yz}$ when compared to those in $\hat{\mathcal{H}}_{xz}$.

The Zeeman splitting term $\hat{\mathcal{H}}_x$ and the dipolar term $\hat{\mathcal{H}}_{xz}$ both generate terms which are linear in $\hat{S}_i^x$. In particular,

$$\hat{\mathcal{H}}_x + \hat{\mathcal{H}}_{xz} = -\Delta\sin\theta\sum_j\hat{S}_j^x + \frac{2\varepsilon_{\rm d}\sin\theta\cos\theta}{S}\sum_j\hat{S}_j^x - \frac{2\varepsilon_{\rm d}\sin\theta\cos\theta}{S}\sum_{j\tau}\frac{\tau_x^2}{\tau^5}\hat{S}_j^x\hat{n}_{j+\tau}. \tag{S61}$$

As a result, we conveniently define θ such that the linear term is cancelled. This leads to

$$\begin{aligned}\cos\theta = \frac{S\Delta}{2\varepsilon_{\rm d}}, &\qquad 0 \le S\Delta \le 2\varepsilon_{\rm d},\\ \theta = 0, &\qquad S\Delta > 2\varepsilon_{\rm d}.\end{aligned} \tag{S62}$$

Therefore, in this case, the terms

$$\hat{\mathcal{H}}_x + \hat{\mathcal{H}}_{xz} = -\frac{2\varepsilon_{\rm d}\sin\theta\cos\theta}{S}\sum_{j\tau}\frac{\tau_x^2}{\tau^5}\hat{S}_j^x\hat{n}_{j+\tau}, \tag{S63}$$

lead to a cubic interaction term only.

In the same spirit, combining $\hat{\mathcal{H}}_z$ from Zeeman splitting and $\hat{\mathcal{H}}_{zz}$ from dipolar interaction, we find

$$\hat{\mathcal{H}}_z + \hat{\mathcal{H}}_{zz} = \left(\Delta S\cos\theta - 2\varepsilon_{\rm d}\cos^2\theta\right)\sum_j\hat{n}_j + \varepsilon_{\rm d}\cos^2\theta\frac{a^3}{\pi}\sum_{j\tau}\frac{\tau_x^2}{\tau^5}\hat{n}_j\hat{n}_{j+\tau}. \tag{S64}$$

As a result, the combination of $\mathcal{H}_z$ and $\mathcal{H}_{zz}$ gives rise to a magnon gap induced by Zeeman splitting and dipolar interactions, and a quartic interaction induced by dipolar interactions.

Effective Hamiltonian

To cast the dipolar Hamiltonian into a long-wavelength, effective Hamiltonian, we use the Holstein-Primakoff transformation to leading order, which results in

$$\sum_{j\tau}\frac{\tau_x^2}{\tau^5}\hat{n}_j\hat{n}_{j+\tau}=\sum_{j\tau}\frac{\tau_x^2}{\tau^5}\hat{a}_j^\dagger\hat{a}_{j+\tau}^\dagger\hat{a}_{j+\tau}\hat{a}_j=\sum_{\boldsymbol{kpq}}\left(\sum_{\tau}e^{-i\boldsymbol{q}\cdot\boldsymbol{\tau}}\frac{\tau_x^2}{\tau^5}\right)\hat{a}_{\boldsymbol{k}+\boldsymbol{q}}^\dagger\hat{a}_{\boldsymbol{p}-\boldsymbol{q}}^\dagger\hat{a}_{\boldsymbol{p}}\hat{a}_{\boldsymbol{k}}\approx\frac{\pi}{a^3}\sum_{\boldsymbol{kpq}}\hat{a}_{\boldsymbol{k}+\boldsymbol{q}}^\dagger\hat{a}_{\boldsymbol{p}-\boldsymbol{q}}^\dagger\hat{a}_{\boldsymbol{p}}\hat{a}_{\boldsymbol{k}}. \tag{S65}$$

In the last step, we used Eq.(S56). In addition, for Eq.(S63), we use

$$\begin{aligned}\sum_{j\tau}\frac{\tau_x^2}{\tau^5}\hat{S}_j^x\hat{n}_{j+\tau}=\sqrt{\frac{S}{2}}\sum_{j\tau}\frac{\tau_x^2}{\tau^5}\left(\hat{a}_j^\dagger\hat{a}_{j+\tau}^\dagger\hat{a}_{j+\tau}+\hat{a}_{j+\tau}^\dagger\hat{a}_{j+\tau}\hat{a}_j\right)&=\sqrt{\frac{S}{2N}}\sum_{\boldsymbol{kp\tau}}\frac{\tau_x^2}{\tau^5}\left[e^{-\boldsymbol{p}\cdot\boldsymbol{\tau}}\hat{a}_{\boldsymbol{p}}^\dagger\hat{a}_{\boldsymbol{k}}^\dagger\hat{a}_{\boldsymbol{k}+\boldsymbol{p}}+e^{-i\boldsymbol{k}\cdot\boldsymbol{p}}\hat{a}_{\boldsymbol{k}+\boldsymbol{p}}^\dagger\hat{a}_{\boldsymbol{p}}\hat{a}_{\boldsymbol{k}}\right]\\&\approx\sqrt{\frac{S}{2N}}\frac{\pi}{a^3}\sum_{\boldsymbol{kp}}\left(\hat{a}_{\boldsymbol{p}}^\dagger\hat{a}_{\boldsymbol{k}}^\dagger\hat{a}_{\boldsymbol{k}+\boldsymbol{p}}+\hat{a}_{\boldsymbol{k}+\boldsymbol{p}}^\dagger\hat{a}_{\boldsymbol{p}}\hat{a}_{\boldsymbol{k}}\right).\end{aligned} \tag{S66}$$

Putting everything together, we find that, at long wavelength, the dipolar and Zeeman Hamiltonian can be effectively written as

$$\begin{aligned}&\hat{\mathcal{H}}_{\rm d}+\hat{\mathcal{H}}_{\rm z}\approx\sum_{\boldsymbol{k}}\left[\Delta\hat{a}_{\boldsymbol{k}}^\dagger\hat{a}_{\boldsymbol{k}}+\lambda_2\left(\hat{a}_{\boldsymbol{k}}\hat{a}_{-\boldsymbol{k}}+\hat{a}_{\boldsymbol{k}}^\dagger\hat{a}_{-\boldsymbol{k}}^\dagger\right)\right]-\frac{\lambda_3}{\sqrt{N}}\sum_{\boldsymbol{kp}}\left(\hat{a}_{\boldsymbol{p}}^\dagger\hat{a}_{\boldsymbol{k}}^\dagger\hat{a}_{\boldsymbol{k}+\boldsymbol{p}}+\hat{a}_{\boldsymbol{k}+\boldsymbol{p}}^\dagger\hat{a}_{\boldsymbol{p}}\hat{a}_{\boldsymbol{k}}\right)+\frac{\lambda_4}{N}\sum_{\boldsymbol{kpq}}a_{\boldsymbol{p}+\boldsymbol{q}}^\dagger\hat{a}_{\boldsymbol{k}-\boldsymbol{q}}^\dagger\hat{a}_{\boldsymbol{p}}\hat{a}_{\boldsymbol{k}},\\&\tilde{\Delta}=\left(\Delta S\cos\theta-2\varepsilon_{\rm d}\cos^2\theta\right)+\frac{\varepsilon_{\rm d}\sin^2\theta}{S},\quad\lambda_2=\frac{\varepsilon_{\rm d}\sin^2\theta}{2S},\quad\lambda_3=\varepsilon_{\rm d}\sqrt{2/S}\sin\theta\cos\theta,\quad\lambda_4=\varepsilon_{\rm d}\cos^2\theta.\end{aligned} \tag{S67}$$

Bogoliubov transformation

For sufficiently small Zeeman fields, the canting angle is $0<\theta\leq\pi/2$, and $\lambda_{2,3}$ are finite. The quadratic part of the Heisenberg Hamiltonian combined with Eq.(S67),

$$\hat{\mathcal{H}}_2=\sum_{\boldsymbol{k}}\left[(\Delta+\varepsilon_{\boldsymbol{k}})\hat{a}_{\boldsymbol{k}}^\dagger\hat{a}_{\boldsymbol{k}}+\lambda_2(\hat{a}_{\boldsymbol{k}}\hat{a}_{-\boldsymbol{k}}+\hat{a}_{\boldsymbol{k}}^\dagger\hat{a}_{-\boldsymbol{k}}^\dagger)\right], \tag{S68}$$

can be diagonalized using a Bogoliubov transformation:

$$\hat{a}_{\boldsymbol{k}}=s_{\boldsymbol{k}}\hat{\beta}_{\boldsymbol{k}}+t_{\boldsymbol{k}}\hat{\gamma}_{-\boldsymbol{k}}^\dagger,\quad\hat{a}_{-\boldsymbol{k}}=s_{\boldsymbol{k}}\hat{\beta}_{\boldsymbol{k}}+t_{\boldsymbol{k}}\hat{\gamma}_{-\boldsymbol{k}}^\dagger, \tag{S69}$$

where $s_{\boldsymbol{k}}$ and $t_{\boldsymbol{k}}$ are $\boldsymbol{k}$-dependent real numbers. It is straightforward to show that

$$s_{\boldsymbol{k}}=\cosh\varphi_{\boldsymbol{k}},\quad t_{\boldsymbol{k}}=\sinh\varphi_{\boldsymbol{k}}, \tag{S70}$$

diagonalizes $\hat{\mathcal{H}}_2$,

$$\hat{\mathcal{H}}_2=\sum_{\boldsymbol{k}}E_{\boldsymbol{k}}\left[\beta_{\boldsymbol{k}}^\dagger\beta_{\boldsymbol{k}}+\gamma_{\boldsymbol{k}}^\dagger\gamma_{\boldsymbol{k}}\right],\quad E_{\boldsymbol{k}}=\sqrt{(\varepsilon_{\boldsymbol{k}}+\Delta)^2-\lambda_2^2}, \tag{S71}$$

where $\varphi_{\boldsymbol{k}}$ is the solution of

$$\sinh 2\varphi_{\boldsymbol{k}}=-\frac{\lambda_2}{2E_{\boldsymbol{k}}}. \tag{S72}$$

Several comments are in order. First, we note that the magnon dispersion is quadratic, with or without dipolar interactions. In particular, in the presence of dipolar interactions, there will be a small correction to the magnon mass at low energies on the order of $\mathcal{O}(\varepsilon_{\rm d}/J)$, and which we will neglect (quadratic dispersion greatly simplifies the hydrodynamic description, as will be discussed below). Second, we are mainly interested on the hydrodynamic behavior at large T such that magnon-magnon collision become important. In the regime $\varepsilon_{\rm d}\ll T\ll J$, most magnons will typically have large kinetic energies $\varepsilon_{\boldsymbol{k}}$ such that corrections due to the Bogoliubov transformation are negligible.

For sufficiently large Zeeman fields, when $\Delta\geq\varepsilon_{\rm d}$ and $\theta=0$, then the coupling terms verigy $\lambda_{2,3}=0$. In this case, the quadratic part of $\hat{\mathcal{H}}_J+\hat{\mathcal{H}}_{\rm d}+\hat{\mathcal{H}}_{\rm z}$ is already diagonal in the $(\hat{a}_{\boldsymbol{k}},a_{\boldsymbol{k}}^\dagger)$ basis and there is no need for a Bogoliubov transformation. Having all these considerations in mind, in our hydrodynamic calculations we set $\lambda_2\to 0$ from the beginning.

Magnon leakage

Three magnon processes in Eq.(S67) do not preserve particle number. This means that the distribution function $\bar{n}_{\boldsymbol{k}}$ in Eq.(9) of the main text is a quasi-equilibrium distribution if $0 < z < 1$. The total magnon leakage rate can be calculated as

$$\frac{dn}{dt} = -\frac{\lambda_3^2}{N^2}\sum_{\boldsymbol{kp}} 2\pi\delta(\varepsilon_{\boldsymbol{k}} + \varepsilon_{\boldsymbol{p}} + \Delta - \varepsilon_{\boldsymbol{k}+\boldsymbol{p}})\left[\bar{n}_{\boldsymbol{k}}\bar{n}_{\boldsymbol{p}}(1+\bar{n}_{\boldsymbol{k}+\boldsymbol{p}}) - (1+\bar{n}_{\boldsymbol{k}})(1+\bar{n}_{\boldsymbol{p}})\bar{n}_{\boldsymbol{k}+\boldsymbol{p}}\right]. \tag{S73}$$

Here we note that three magnon processes are not necessarily suppressed by energy and momenta conservation. For instance, if the incoming magnon states have momenta that verifies $\boldsymbol{k}\cdot\boldsymbol{p} = m\Delta$, then energy and momentum is conserved after the collision. For concreteness, let us assume that $u_\alpha \ll \sqrt{T/m}$, which leads to

$$\frac{dn}{dt} = -\frac{\gamma_{\mathrm{leak}}(z^2 - z^3)}{4\pi}\frac{T\lambda_3^2}{J^2a^2}, \quad \gamma_{\mathrm{leak}} = \frac{16\pi}{z^3}\int\frac{d\tilde{\boldsymbol{k}}}{(2\pi)^2}\int\frac{d\tilde{\boldsymbol{p}}}{(2\pi)^2}\delta[\tilde{\boldsymbol{k}}^2 + \tilde{\boldsymbol{p}}^2 + \tilde{\Delta} - (\tilde{\boldsymbol{k}}+\tilde{\boldsymbol{p}})^2]\bar{n}_{\tilde{\boldsymbol{k}}}\bar{n}_{\tilde{\boldsymbol{p}}}\bar{n}_{\tilde{\boldsymbol{k}}+\tilde{\boldsymbol{p}}}e^{\tilde{\boldsymbol{k}}^2+\tilde{\boldsymbol{p}}^2}, \tag{S74}$$

where we normalized $\tilde{\boldsymbol{k}} = \boldsymbol{k}/k_{\mathrm{th}}$. Similarly to the collision integral in Eq.(S25), $\gamma_{\mathrm{leak}}(z)$ can be shown to be $\gamma_{\mathrm{leak}} \sim \mathcal{O}(1)$. From here we can define the leakage rate

$$\frac{1}{\tau_{\mathrm{leak}}} = \frac{1}{n}\frac{dn}{dt} = \frac{\gamma_{\mathrm{leak}}\lambda_3^2}{2J}(z^2 - z^3). \tag{S75}$$

Using $J \sim 1000\,\mathrm{K}$, $\lambda_3 \sim 1\,\mathrm{K}$, and $z \approx 0.9$, we obtain $1/\tau_{\mathrm{leak}} \sim 5\,\mathrm{MHz}$. As such, magnon number can be assumed to be a good conserved quantity for the GHz frequencies of interest.